

Photon-photon and photo-nuclear collisions at CERN

C.A. Bertulani

Department of Physics and Astronomy
Texas A&M University-Commerce



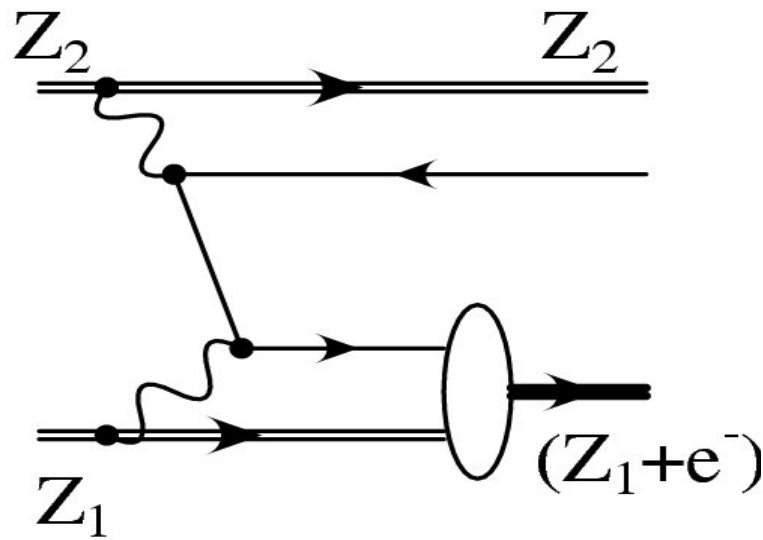
Gerhard Baur, IKP-Juelich & U. Basel

Pair Production with Capture

CB, Baur, Phys. Rep. 163, 299 (1988)

$$\sigma \propto \frac{Z_P^2 Z_T^6 \alpha^8}{m_e^2} \left[\ln\left(\frac{0.68 \gamma}{2}\right) - \frac{5}{3} \right]$$

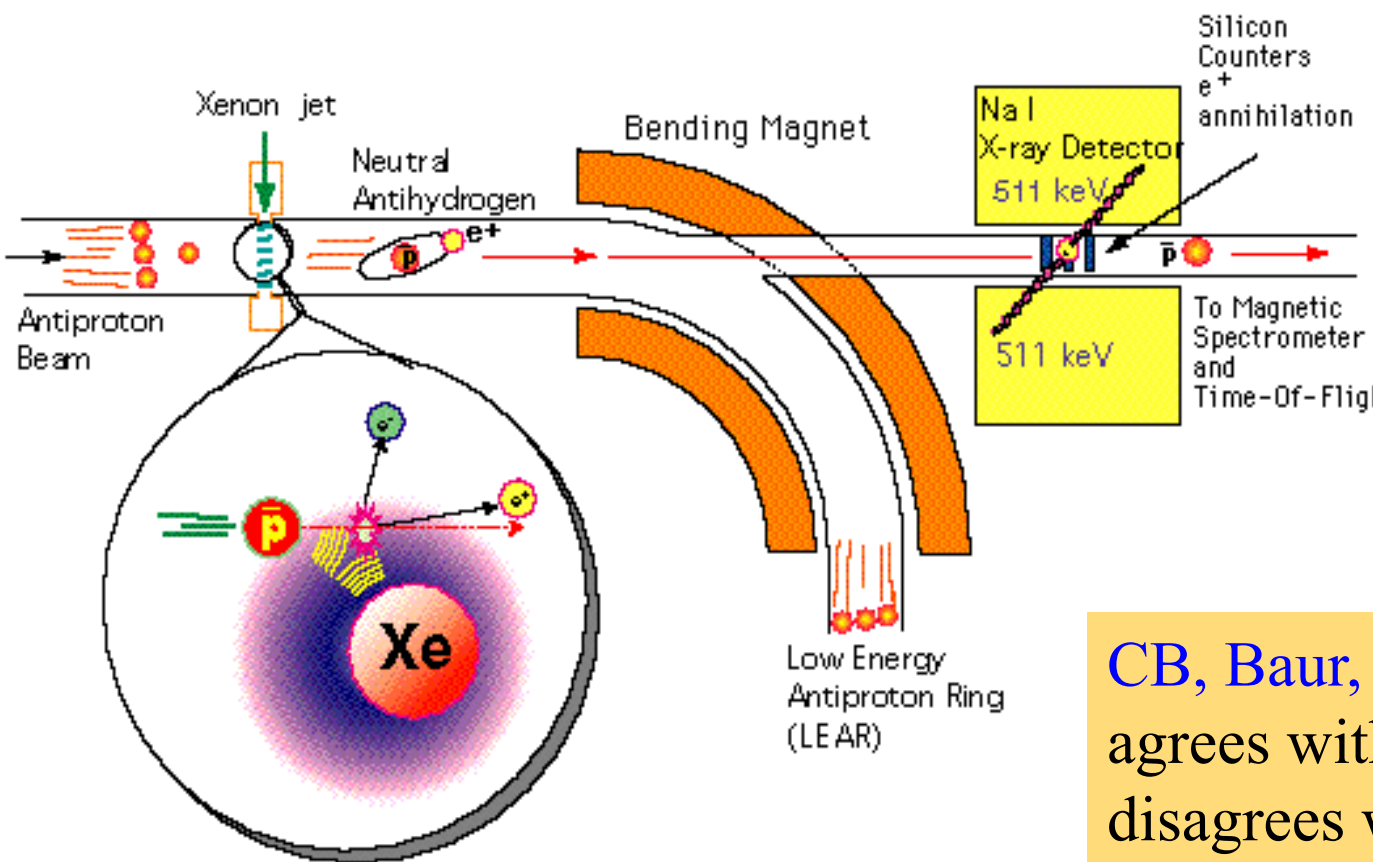
~ 300 b for Pb+Pb at LHC



Production of anti-H

CERN: Baur et al, PLB 368, 251 (1996)

Fermilab: G. Blanford et al, PRL 80, 3037 (1998)



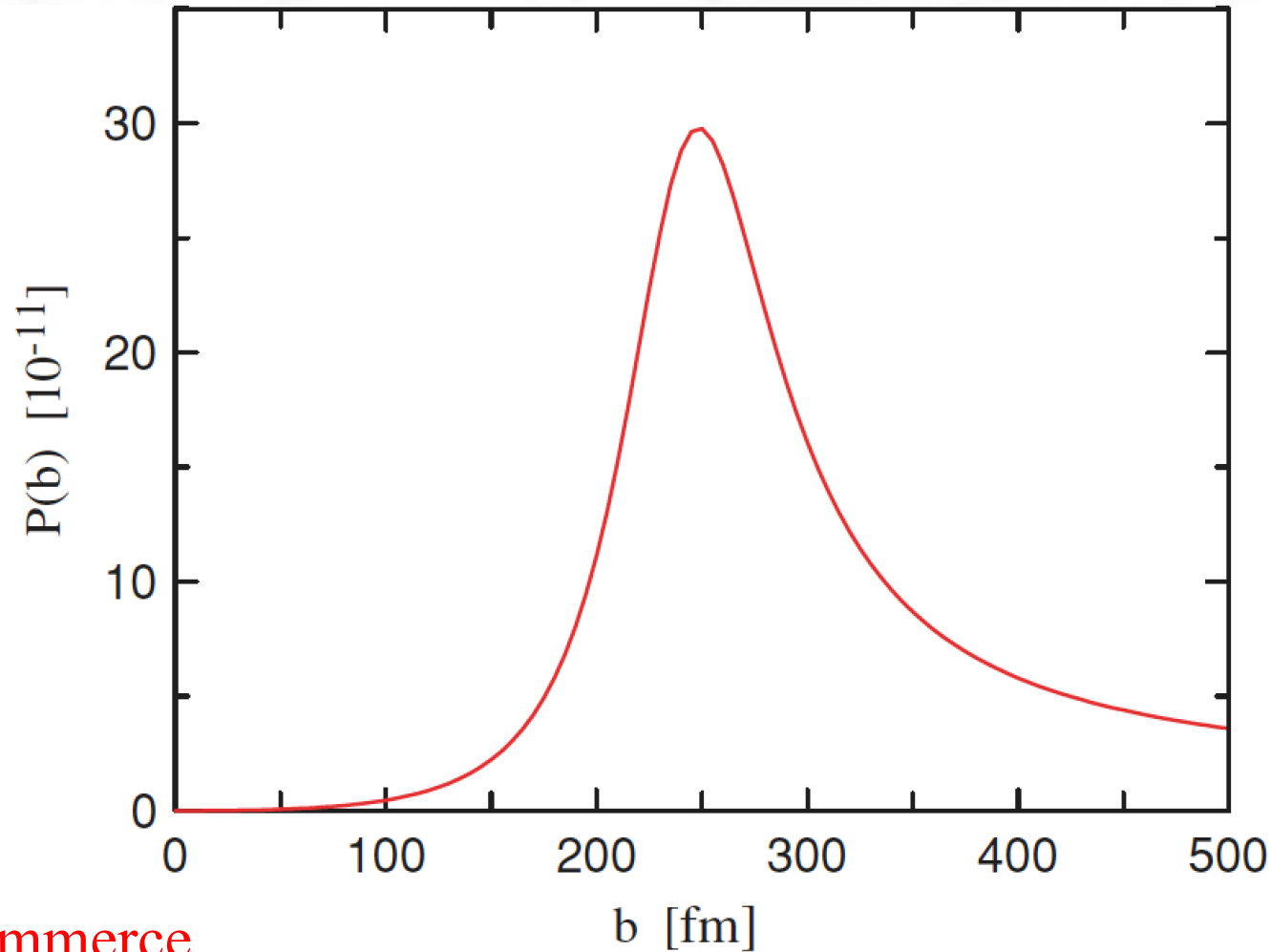
CB, Baur, PRD 58, 034005 (1998)
 agrees with Fermilab data but
 disagrees with CERN (10 x)

Production of Exotic Atoms



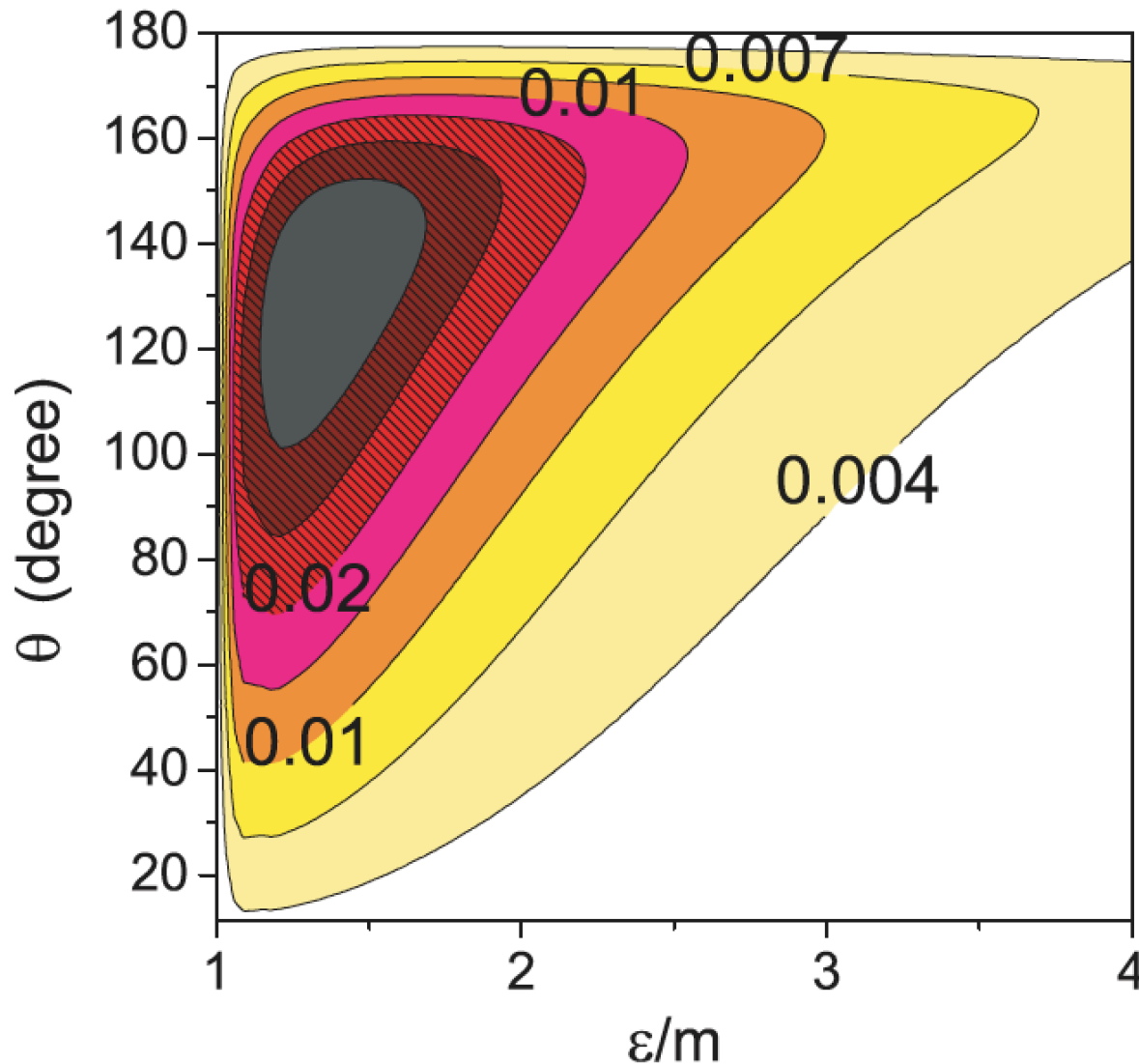
Mark Ellermann

Texas A&M University-Commerce



Probability of muonic atom production in pp collisions at the LHC as a function of the impact parameter.

Production of Exotic Atoms



Contour plot with the angular distribution of the positive muon when the negative muon is captured by a proton at the LHC, as a function of the angle that the free muon has with the direction of motion of the muonic atom and of the energy of the free positive muon.

Production of Exotic Atoms

CB, Ellermann, PRC 81, 044910 (2010)

“Exotic” atom	γp	γA
Hydrogen	63.4	132 b
muonic	44.8×10^{-4}	0.16 mb
pionic	21.3×10^{-4}	0.09 mb
kaonic	1.3×10^{-4}	4.3 μ b
ρ atom	0.51×10^{-4}	1.3 μ b
protonium	0.09×10^{-4}	0.5 μ b

Cross sections for production of exotic atoms in pp and PbPb collisions at the CERN Large Hadron Collider (LHC).

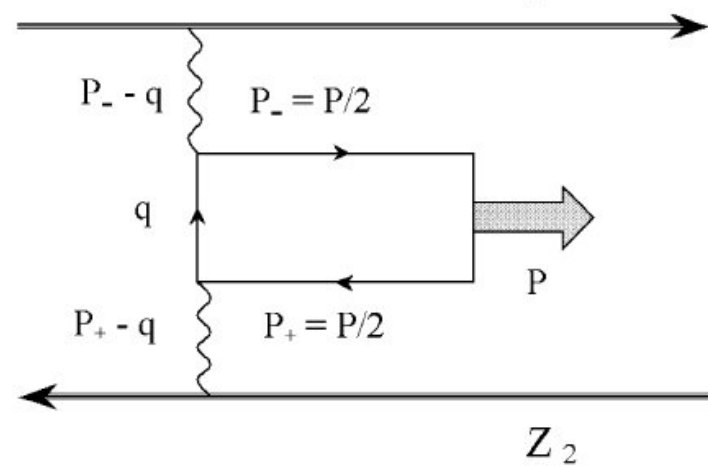
QFT with Bound states

Spin 0,2, C=even

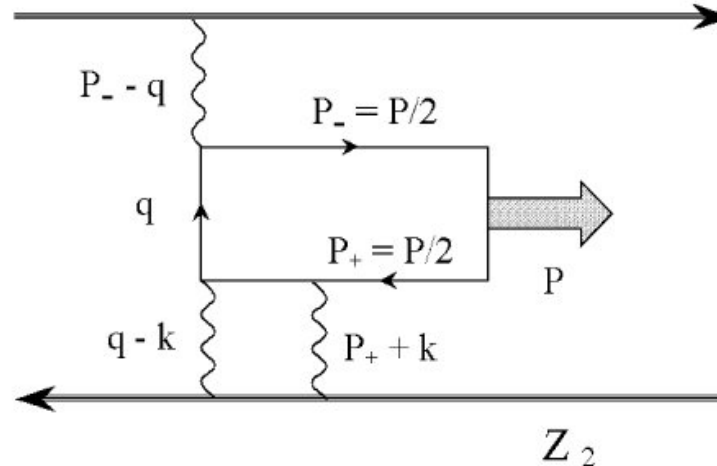
Z_1

Spin 1, C=odd

Z_1



(a)



(b)



Fernando Navarra
University of São Paulo

$$\mathcal{M} = -ie^2 \bar{u}\left(\frac{P}{2}\right) \left[\int \frac{d^4 q}{(2\pi)^4} \mathcal{A}^{(1)}\left(\frac{P}{2} - q\right) \frac{\not{q} + m}{q^2 - m^2} \right. \\ \left. \times \mathcal{A}^{(2)}\left(\frac{P}{2} + q\right) + \mathcal{A}^{(1)}\left(\frac{P}{2} + q\right) \frac{\not{q} + m}{q^2 - m^2} \mathcal{A}^{(2)}\left(\frac{P}{2} - q\right) \right] v\left(\frac{P}{2}\right)$$

Bodwin, Yennie, Gregorio,
Rev. Mod. Phys. 57, 723 (1985)

CB, Navarra, NPA703 (2002) 861

Spin 0

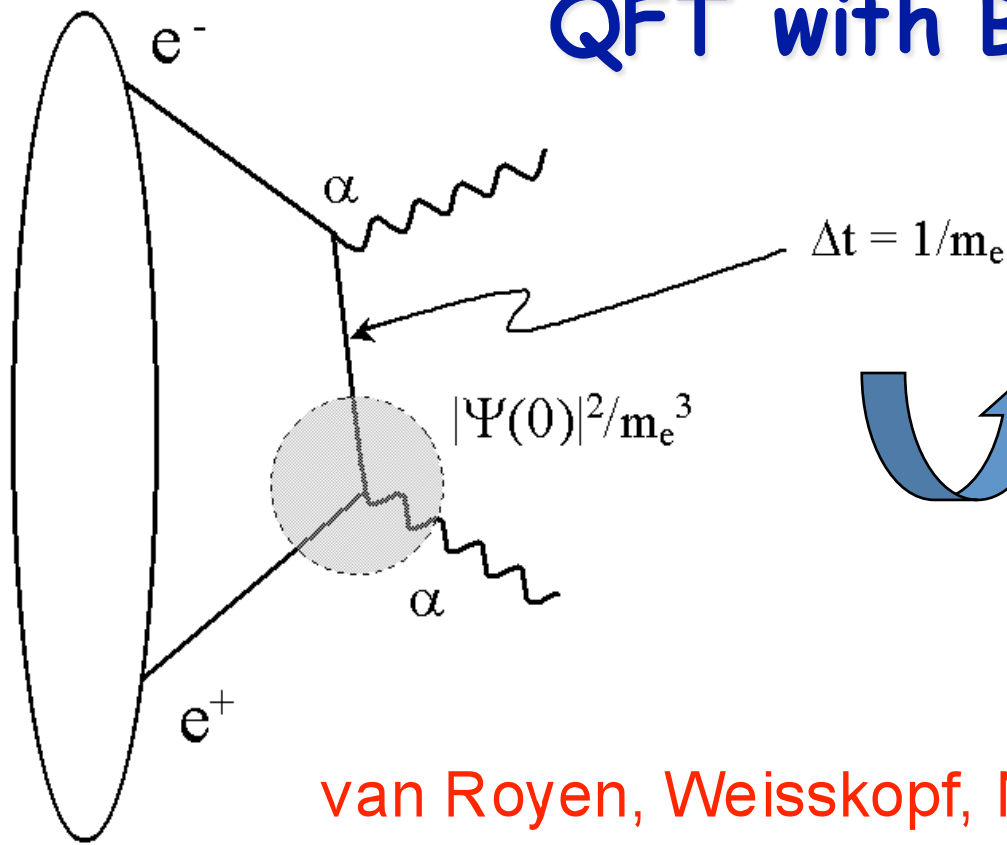
$$\bar{u}Bv \longrightarrow \sqrt{2M} \operatorname{tr} \left(\frac{B}{\sqrt{2}} \right) \Psi(0)$$

Spin 1

$$\bar{u}Bv \longrightarrow \sqrt{2M} \operatorname{tr} \left(\frac{\hat{\epsilon} \cdot \sigma}{\sqrt{2}} B \right) \Psi(0)$$

Example: parapositronium ($S = 0$) and orthopositronium ($S = 1$)

QFT with Bound states



$$\Gamma \sim \alpha^2 |\Psi(0)|^2 / m_e^2$$

RECIPE

- replace electrons by quarks
- get rid of $|\psi(0)|^2$

van Royen, Weisskopf, Nuovo Cimento A 50, 617 (1967)
 Appelquist, Politzer, PRL 34, 365 (1975)

$$\Gamma_{\gamma\gamma}^{J=0} = \frac{48\pi\alpha^2}{M^2} |\Psi(0)|^2 \sum_i Q_i^4$$

$$\Gamma_{\gamma\gamma}^{(J=2)} = (2J + 1) \Gamma_{\gamma\gamma}^{(J=0)} = 5 \Gamma_{\gamma\gamma}^{(J=0)}$$

Example: parapositronium ($S = 0$) at LHC

$$|\Psi(0)|^2 = (m_e \alpha)^3 / 8\pi n^3$$



$$\sigma = 325 \text{ mb}$$

Study of positronium propagation in thin metals:
 QFT for bound states

QFT with bound states at CERN

$$\sigma_X = \int d\omega_1 d\omega_2 n_\gamma(\omega_1) n_\gamma(\omega_2) \sigma_{\gamma\gamma}^X(\omega_1 \omega_2 s)$$

$$n(\omega, b) = \frac{2Z^2 \alpha \omega^2}{\pi \gamma^2} \int_0^\infty db b \left[K_1^2(\xi) + \frac{1}{\gamma^2} K_0^2(\xi) \right] \exp \left\{ -\sigma_{NN} \int_{-\infty}^\infty dz' \int d^3r \rho(\mathbf{r}) \rho(\mathbf{r}' - \mathbf{r}) \right\}$$

$$\xi = \frac{\omega b}{\gamma c}$$

No need for minimum impact parameter

$$\frac{dn}{d\omega} = 2\pi \int db b \int_0^R dr r \int_0^{2\pi} d\phi \frac{d^3 n(\omega, b + r \cos \phi)}{d\omega d^2 b}$$

Baur, Baron,
NPA 561, 628 (1993)

For meson production at CERN use above in conjunction with

Low, Phys. Rev. 120, 582 (1960)

$$\sigma_{\gamma\gamma}^X(x_1 x_2 s) = 8\pi^2 (2J + 1) \frac{\Gamma_{m_X \rightarrow \gamma\gamma}}{m_X} \delta(x_1 x_2 s - m_X^2)$$

Comment on Joakim Nystrand's Equivalent Photon Spectrum

Low Energies

$$n_{E2} \gg n_{E1} \gg n_{M1} = \beta^2 n_{E1}$$

High Energies

$$n_{E2} \approx n_{E1} \approx n_{M1}$$

Very High Energies (CERN)

$$n_{E2} = n_{E1} = n_{M1}$$

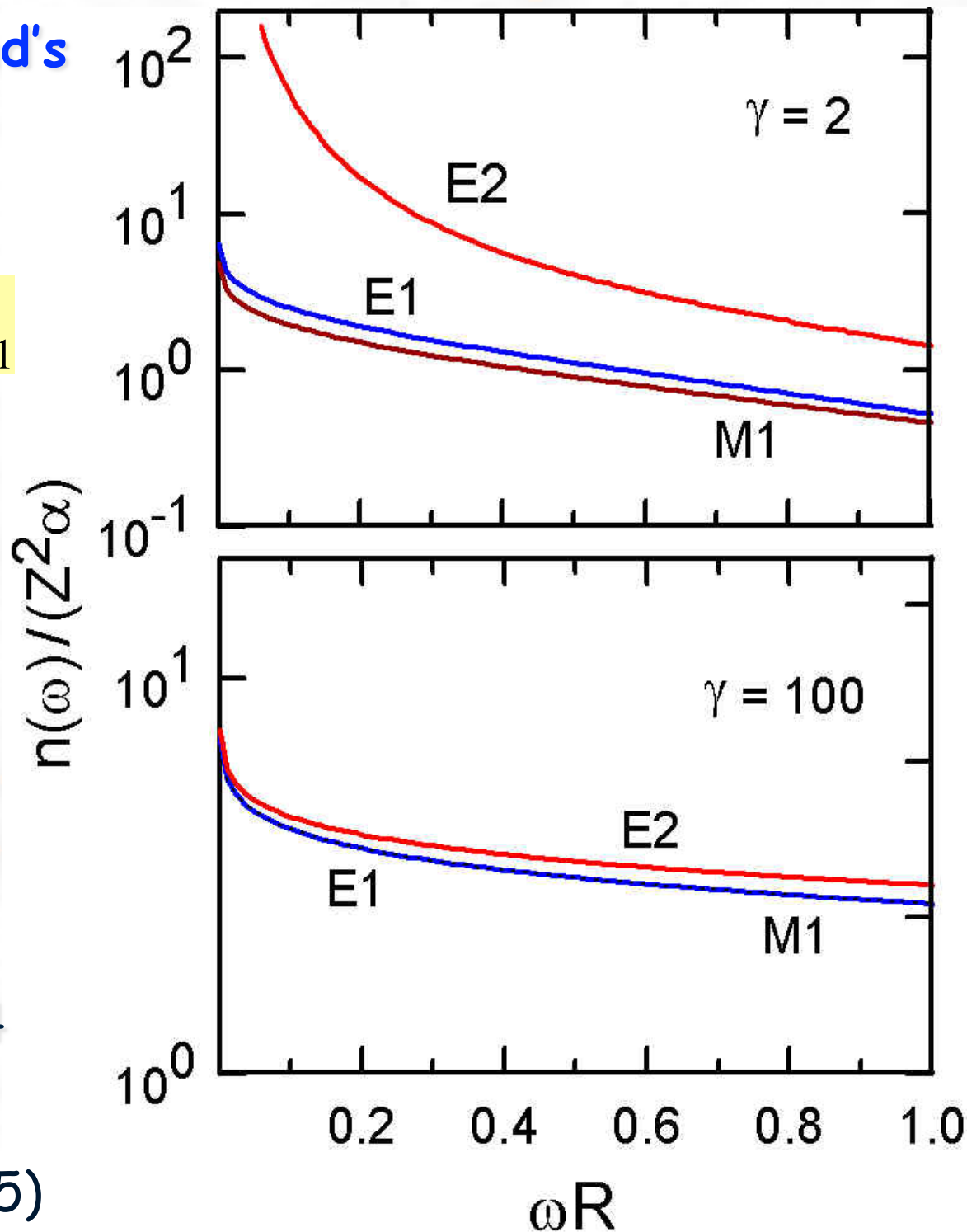
Fermi, 1924

Weizsaecker, Williams, 1934

Improved theory:

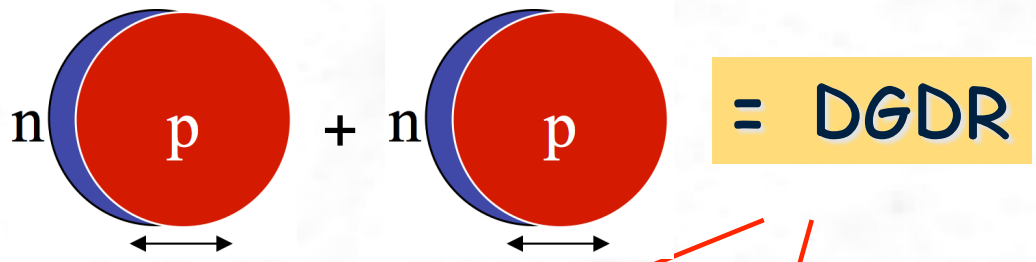
CB, Baur, NPA 442, 739 (1985)

Phys. Rep. 163, 299 (1988)



Comment on Multiple Giant Resonances: Pshenichnov, Strikman

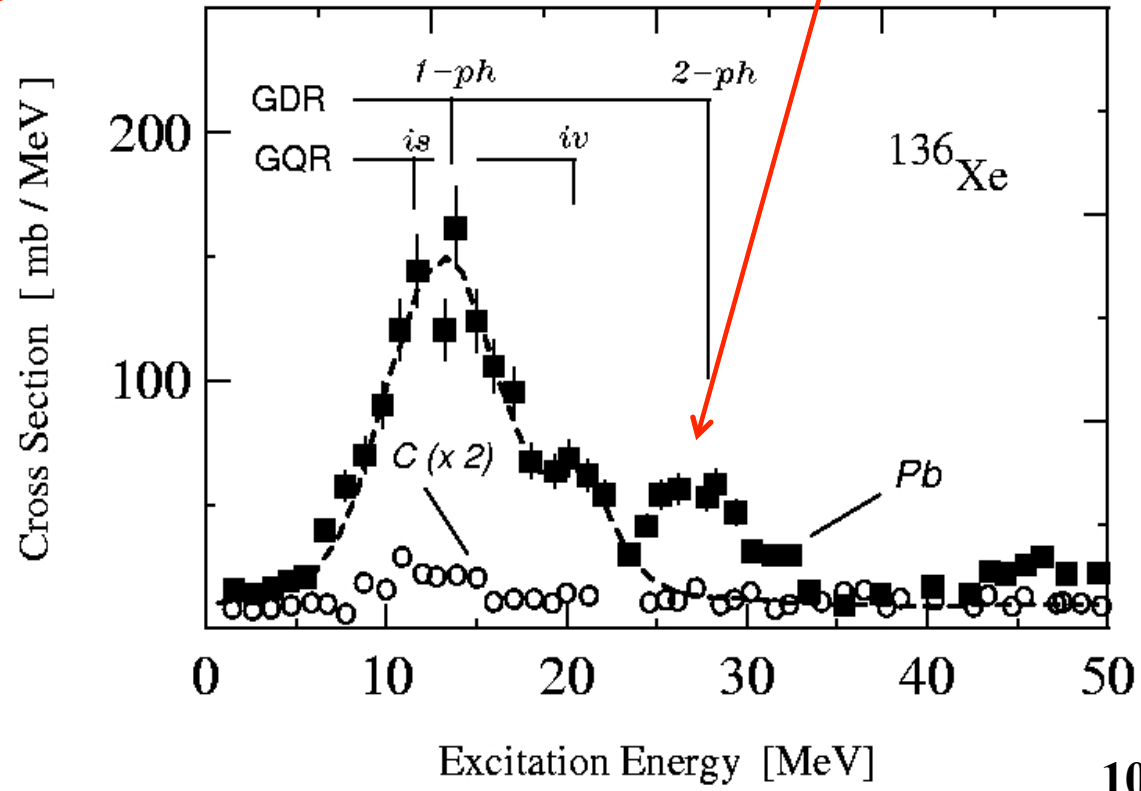
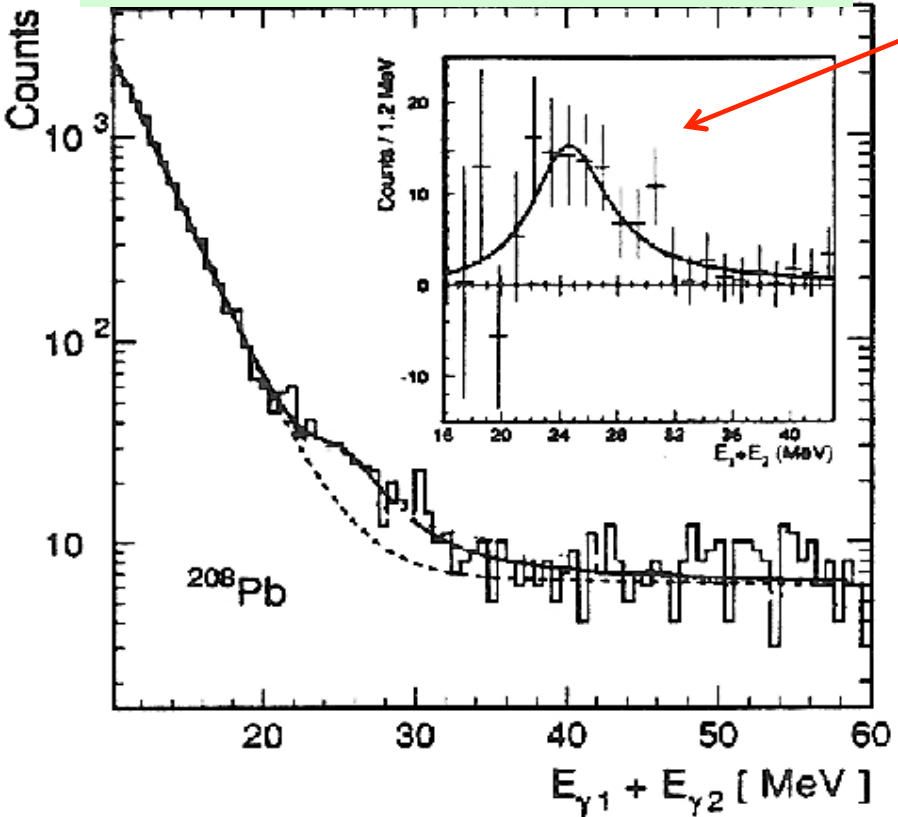
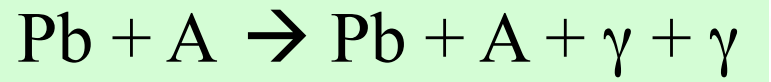
CB, Baur, PLB 174 (1986) 23 1986



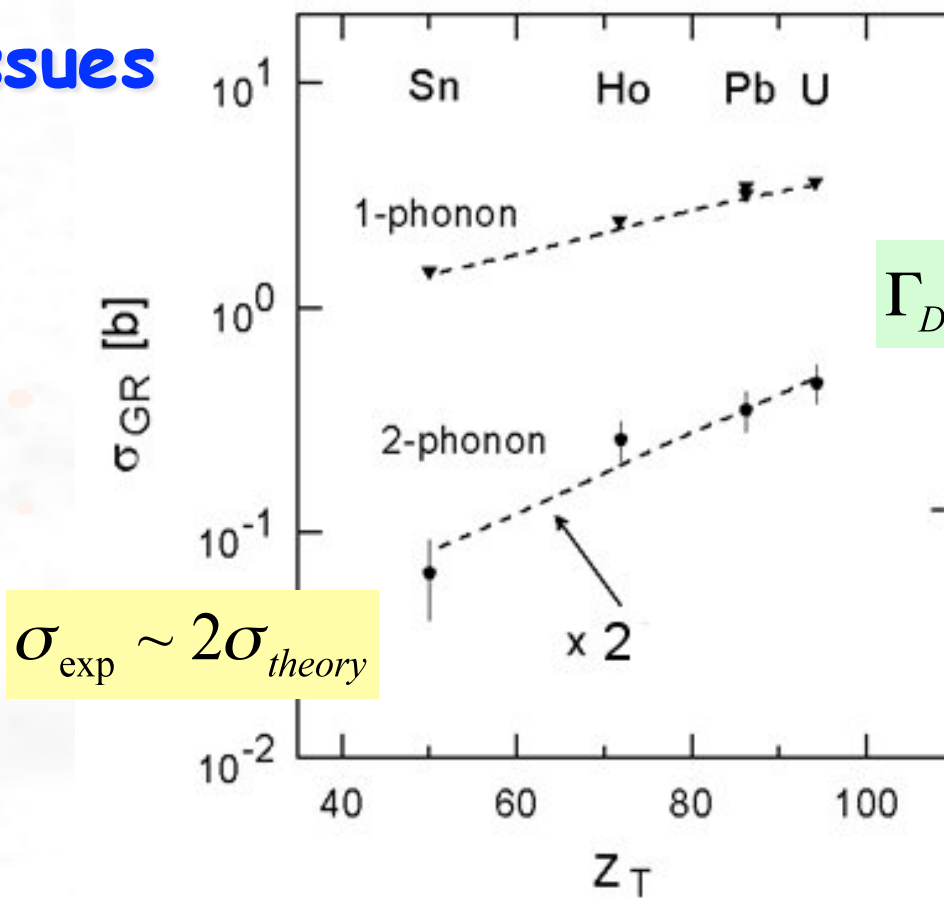
Experiments: GSI ~ 2 GeV/A

Ritman et al 1993 PRL 70 2659 (1993)

Schmidt et al., PRL 70, 1767 (1993)



Open issues

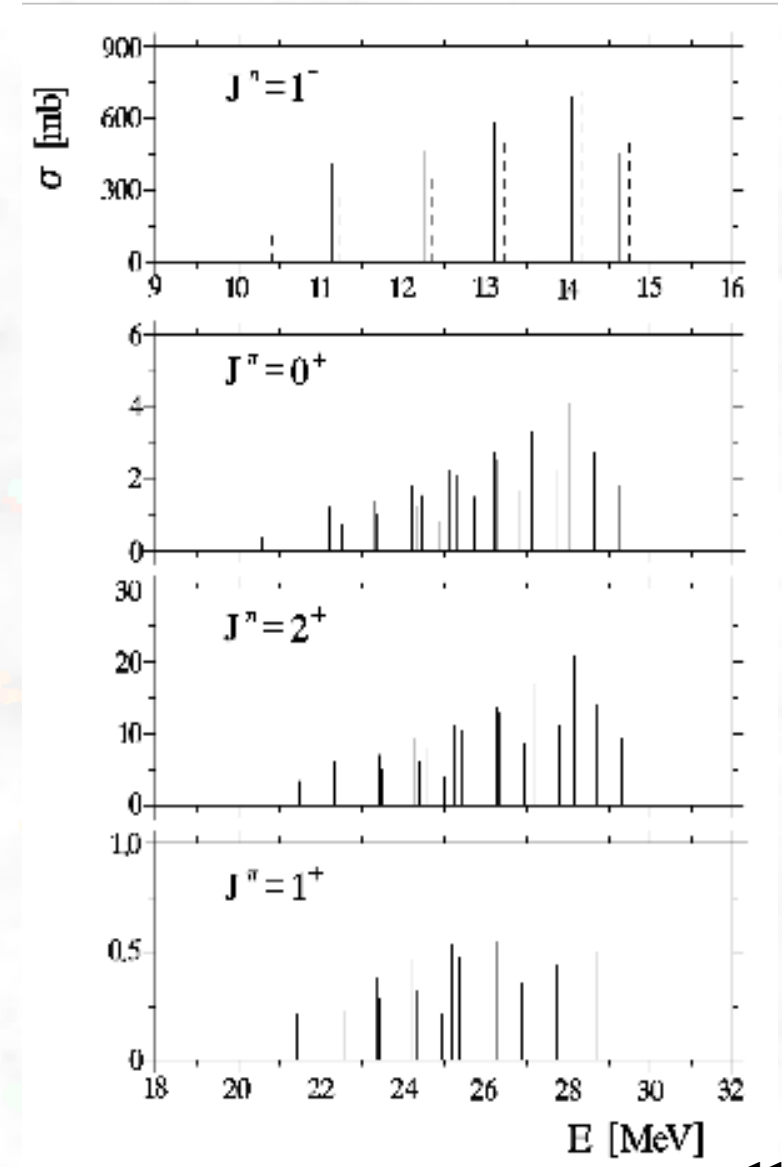
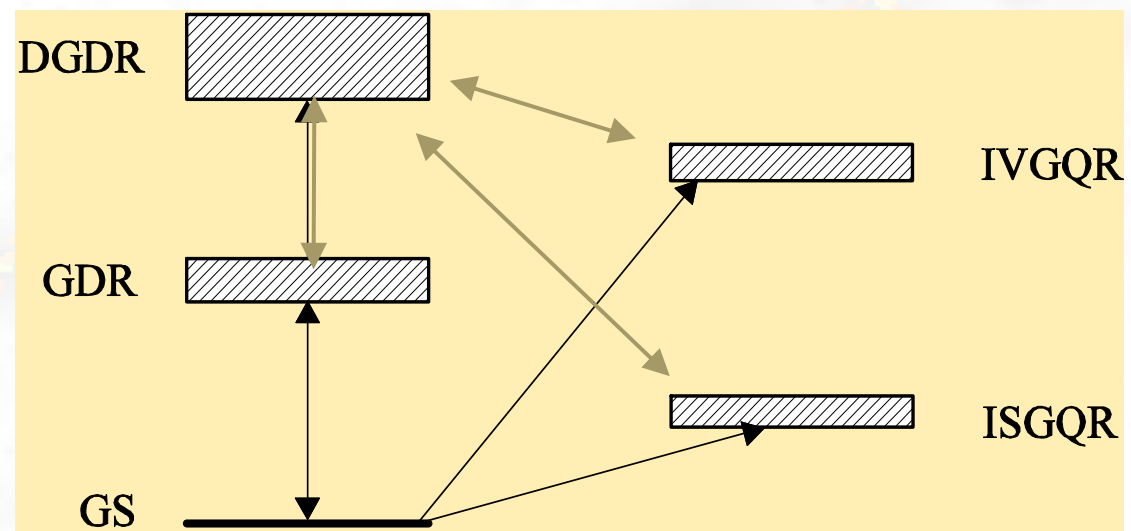


$\sigma_{exp} \sim 2\sigma_{theory}$

Data: GSI (Aumann et al)

$\Gamma_{DGDR} = 2\Gamma_{GDR}$ or $\sqrt{2}\Gamma_{GDR}$?

CB, Ponomarev, Phys. Rep. 321, 139 (1999)
RPA + coupled channels



Testing Widths of various Mesons at CERN

CB, PRC 79, 047901 (2009)

Mesons	J^{PC}	$\Gamma_{\gamma\gamma}^{\text{th}}$ (keV)	$\Gamma_{\gamma\gamma}^{\text{exp}}$ (keV)	Obs.	$\sigma_{\gamma\gamma}^X$
$a_0^{K\bar{K}}$ (980)	(0^{++})	0.6	0.30 ± 0.10	$\rightarrow K\bar{K} \rightarrow \gamma\bar{\gamma}$	3.1 mb
$a_0^{q\bar{q}}$ (980)		1.5		Hypothetical, NR q-model	8.6 mb
$a_0^{q\bar{q}}$ (980)		1.0		Hypothetical, R q-model	5.5 mb
$f_0^{K\bar{K}}$ (980)	(0^{++})	0.6	$0.29^{+0.07}_{-0.09}$	$\rightarrow K\bar{K} \rightarrow \gamma\bar{\gamma}$	3.1 mb
$f_0^{q\bar{q}}$ (980)		4.5		Hypothetical, NR q-model	25.8 mb
$f_0^{q\bar{q}}$ (980)		2.5		Hypothetical, R q-model	14.3 mb
f_0 (1200)		3.25–6.46	Unknown	For $m_q = 0.33$ to 0.22 GeV	9.6–21 mb
f_2 (1274)	(2^{++})	1.75–4.04	2.6 ± 0.24	$\Gamma_{\gamma\gamma}(f_0) / \Gamma_{\gamma\gamma}(f_2) = 1.86\text{--}1.60$	21–49 mb
$f_2^{\lambda=2}$ (1274)		1.71–3.93		$(\lambda = 0) / (\lambda = 2) = 0.022\text{--}0.029$	20–44 mb
$f_2^{\lambda=0}$ (1274)		0.04–0.11			0.09–0.23 mb
f_0 (1800)		2.16–2.52	Unknown	$2^3 P_0$ radial excitation	2.5–3.1 mb
f_2 (1800) ($\lambda = 2$)		1.53–2.44		$2^3 P_2$ radial excitation	1.7–2.9 mb
f_2 (1800) ($\lambda = 0$)		0.08–0.16		"	0.08–14 mb
f_2 (1525)	(2^{++})	0.17	0.081 ± 0.009	$s\bar{s}$, $m_s = 0.55$ GeV fixed	0.86 mb
f_2' (1525) ($\lambda = 0$)		0.065		"	0.21 mb
f_2' (1525) ($\lambda = 2$)		0.9×10^{-3}		"	0.42 μb
f_4 (2050)		0.36–1.76	Unknown	$^3 F_4$	0.03–0.14 mb
f_4 (2050) ($\lambda = 2$)		0.33–1.56		"	0.02–0.13 mb
f_4 (2050) ($\lambda = 0$)		0.03–0.20		"	2–12 μb
f_3 (2050)		0.50–2.49	Unknown	$^3 F_3$	0.03–0.13 mb
f_2 (2050)		2.48–11.11	Unknown	$^3 F_2$	0.12–0.53 mb
f_2 (2050) ($\lambda = 2$)		1.85–8.49		"	0.09–0.46 mb
f_2 (2050) ($\lambda = 0$)		0.63–2.62		"	0.01–0.07 mb
$f_0^{K^*K^*}$ ($\simeq 1750$)		$\simeq 0.05\text{--}0.1$	Unknown	Vector-vector molecule	0.19 mb

Testing Widths of various Mesons at CERN

Mesons	J^{PC}	$\Gamma_{\gamma\gamma}^{\text{th}}$ (keV)	$\Gamma_{\gamma\gamma}^{\text{exp}}$ (keV)	Obs.	$\sigma_{\gamma\gamma}^X$
η_c	(0^{-+})	3.4–4.8	$6.7^{+0.9}_{-0.8}$	$m_c = 1.4\text{--}1.6$ GeV	0.26–0.34 mb
$\eta_c(3790)$		1.85–8.49	1.3 ± 0.6	$m_c = 1.4$ GeV	0.06–0.1 mb
$\eta'_c(3790)$		3.7	Unknown	$m_c = 1.4$ GeV	0.11 mb
$\eta_c(4060)$		3.3	Unknown		0.09 mb
$\eta_{c2}^{1D}(3840)$		$20. \times 10^{-3}$	Unknown		0.15 μb
$\eta_{c2}^{2D}(4210)$		$35. \times 10^{-3}$	Unknown		0.14 μb
$\eta_{c4}^{1G}(4350)$		0.92×10^{-3}	Unknown		0.08 μb
χ_2	(2^{++})	0.56	0.258 ± 0.019	$(\lambda = 2) / (\lambda = 0) = 0.005$	82 μb
χ_0	(0^{++})	1.56	0.276 ± 0.033	$\Gamma_{\gamma\gamma}(\chi_0) / \Gamma_{\gamma\gamma}(\chi_2) = 2.79$	0.05 mb
χ'_2	(2^{++})	0.64	Unknown		0.09 mb
$h_{c2}(3840)$		20×10^{-3}	Unknown	1D_2	82 μb
$\chi_2(4100)$		30×10^{-3}	Unknown	3F_2	0.11 μb

Mesons	J^{PC}	$\Gamma_{\gamma\gamma}^{\text{th}}$ (keV)	$\Gamma_{\gamma\gamma}^{\text{exp}}$ (keV)	Obs.	$\sigma_{\gamma\gamma}^X$
$\eta_b^{1S}(9400)$		0.17×10^{-3}	Unknown		19 nb
$\eta_b^{2S}(9400)$		0.13×10^{-3}	Unknown		16 nb
$\eta_b^{3S}(9480)$		0.11×10^{-3}	Unknown		14 nb
$\eta_{b2}^{1D}(10150)$		$33. \times 10^{-6}$	Unknown		0.4 nb
$\eta_{b2}^{2D}(10450)$		$69. \times 10^{-6}$	Unknown		0.8 nb
$\eta_{b4}^{1G}(10150)$		$59. \times 10^{-6}$	Unknown		0.7 nb
$\eta_b(9366)$	(0^{-+})	0.17	Unknown		0.12 μb
η'_b		0.13	Unknown		0.17 μb
η''_b		0.11	Unknown	$s\bar{s}, m_s = 0.55$ GeV fixed	0.15 μb
$\chi_{b2}(9913)$	(2^{++})	3.7×10^{-3}	Unknown		0.09 μb
$\chi_{b0}(9860)$	(0^{++})	$13. \times 10^{-3}$	Unknown		0.08 μb

Testing Widths of various Mesons at CERN

	J^{PC}	$\Gamma_{\gamma\gamma}^{\text{th}}$ (keV)	$\Gamma_{\gamma\gamma}^{\text{th}}$ (keV)	Cross section (mb)
π_0	(0^{-+})	$3.4 - 6.4 \times 10^{-3}$	$8.4 \pm 0.6 \times 10^{-3}$	27 – 52
π (1300)	(0^{-+})	0.43 – 0.49	unknown	0.69 – 0.71
π (1880)		0.74 – 1.0	unknown	0.8 - 1.1
π_2 (1670)	(2^{-+})	0.11 – 0.27	< 0.072	0.41 – 1.1
π_2 (2130)	2^{-+}	0.10 – 0.16	unknown	0.36 – 0.54
π_2 (2330)		0.21 – 1.6	unknown	0.04 – 0.31



Needs a dedicated experimental collaboration

Parton Distribution Functions (PDFs)

- HERA: $W_{\gamma p} \sim 200 \text{ GeV}$ LHC: $W_{\gamma p} \sim 1 \text{ TeV}$

• Gonçalves, CB, PRC 65, 054905 (2002)

“Peripheral heavy ion collisions as a
probe of the nuclear gluon distribution”

Los Alamos posted in 10/29/2001



Victor Gonçalves
Federal University of Pelotas

$$\sigma_{\gamma g \rightarrow c\bar{c}}(s) = \int_{2m_c}^{\sqrt{s}} dM_{c\bar{c}} \frac{d\sigma_{c\bar{c}}}{dM_{c\bar{c}}} g_A(x, \mu)$$

$$\frac{d\sigma_{\gamma g \rightarrow c\bar{c}}}{dM_{c\bar{c}}} = \frac{4\pi\alpha_s e_c^2}{M_{c\bar{c}}^2} \left[\left(1 + \varepsilon - \frac{1}{2}\varepsilon^2 \right) \ln \left(\frac{1 + \sqrt{1 - \varepsilon}}{1 - \sqrt{1 - \varepsilon}} \right) - (1 + \varepsilon)\sqrt{1 - \varepsilon} \right]$$

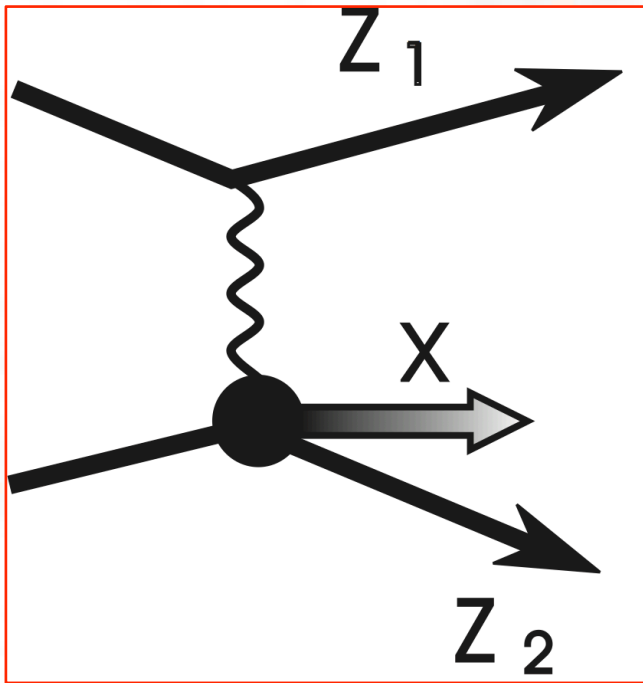
Glueck, Reya, Phys. Lett. 79, 453 (1978)

$$m_c = 1.45 \text{ GeV}$$

$$\varepsilon = \frac{4m_c^2}{M_{c\bar{c}}^2}$$

Parton Distribution Functions at the LHC

$$\sigma(AA \rightarrow XXq\bar{q}) = \int \frac{d\omega}{\omega} n(\omega) \otimes \sigma_{\gamma g \rightarrow q\bar{q}} \otimes xG_A(x, Q^2)$$



$$\gamma_c = 2\gamma_{\text{lab}}^2 - 1$$

Bjorken

$$x = \frac{M}{2p} e^{-y} \ll 1$$

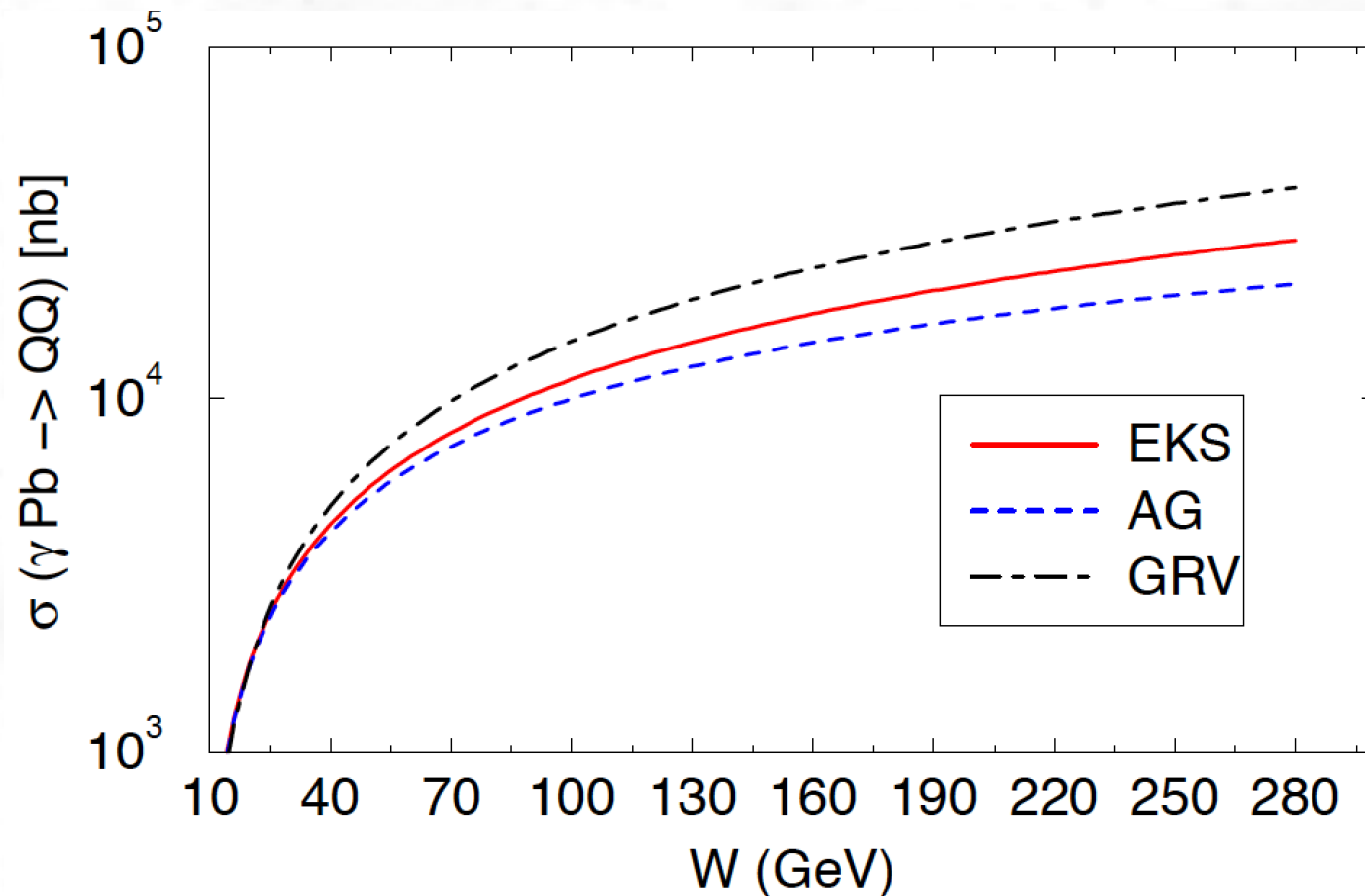
No medium corrections

$$xG_A(x, Q^2) = A \otimes xG_N(x, Q^2)$$

medium corrections

$$xG_A(x, Q^2) = R_G \otimes xG_N(x, Q^2)$$

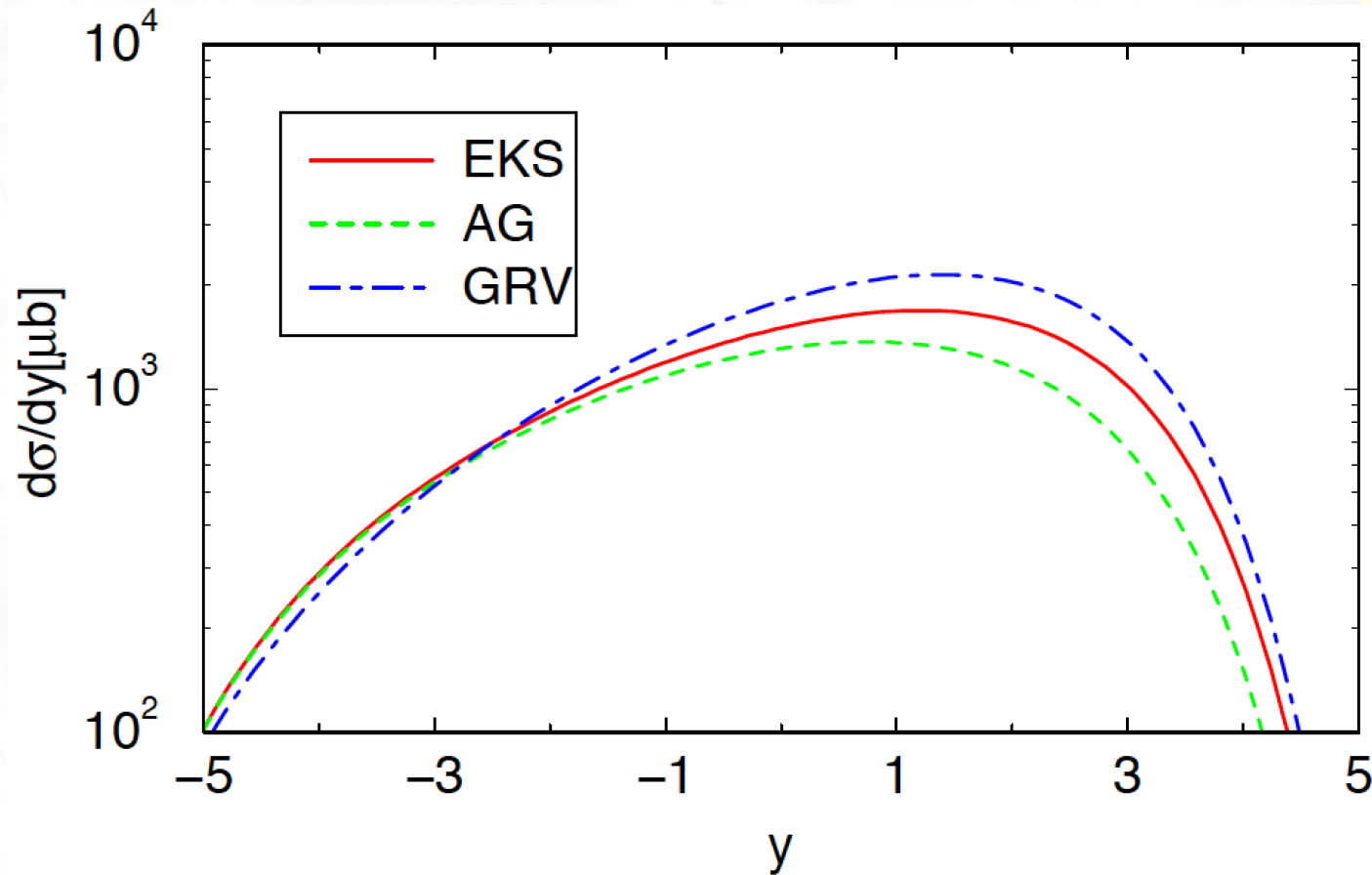
Parton Distribution Functions at the LHC



Energy dependence of the photoproduction of heavy quarks for distinct nuclear gluon distributions ($A = 208$).

- EKS = Eskola, Kolhinen, Salgado, EPJ. C9, 61 (1999)
- AG = Ayala, Gonçalves, EPJ. C 20, 343 (2001)
- GRV = Glück, Reya, Vogt, Z. Phys. C67, 433 (1995)

Parton Distribution Functions at CERN



Rapidity distribution for the photoproduction of charm quarks in $^{208}\text{Pb} + ^{208}\text{Pb}$ collisions at the LHC.

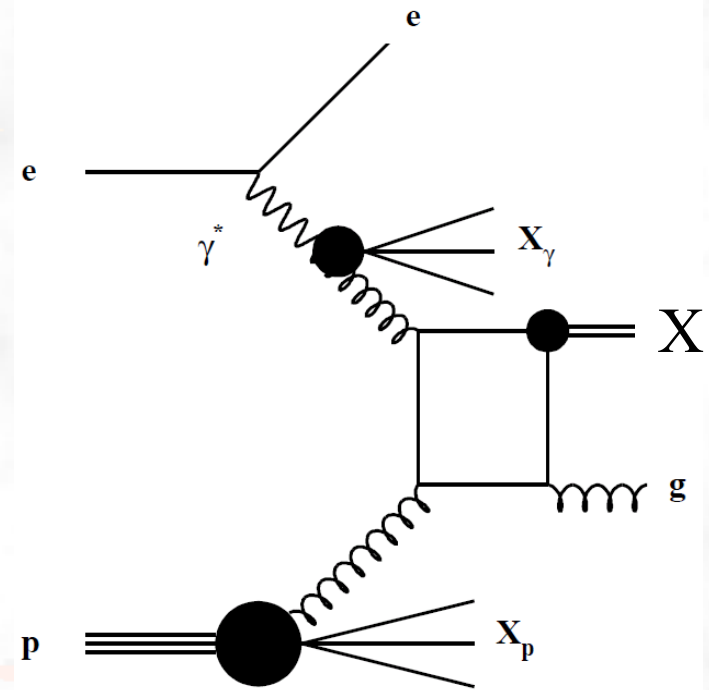
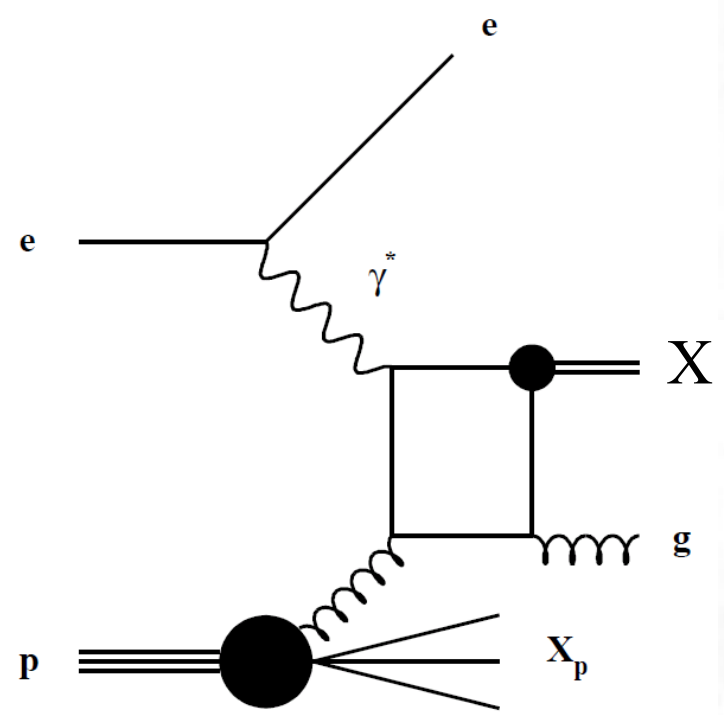
- EKS = Eskola, Kolhinen, Salgado, EPJ. C9, 61 (1999)
- AG = Ayala, Gonçalves, EPJ. C 20, 343 (2001)
- GRV = Glück, Reya, Vogt, Z. Phys. C67, 433 (1995)

Resolved Photons

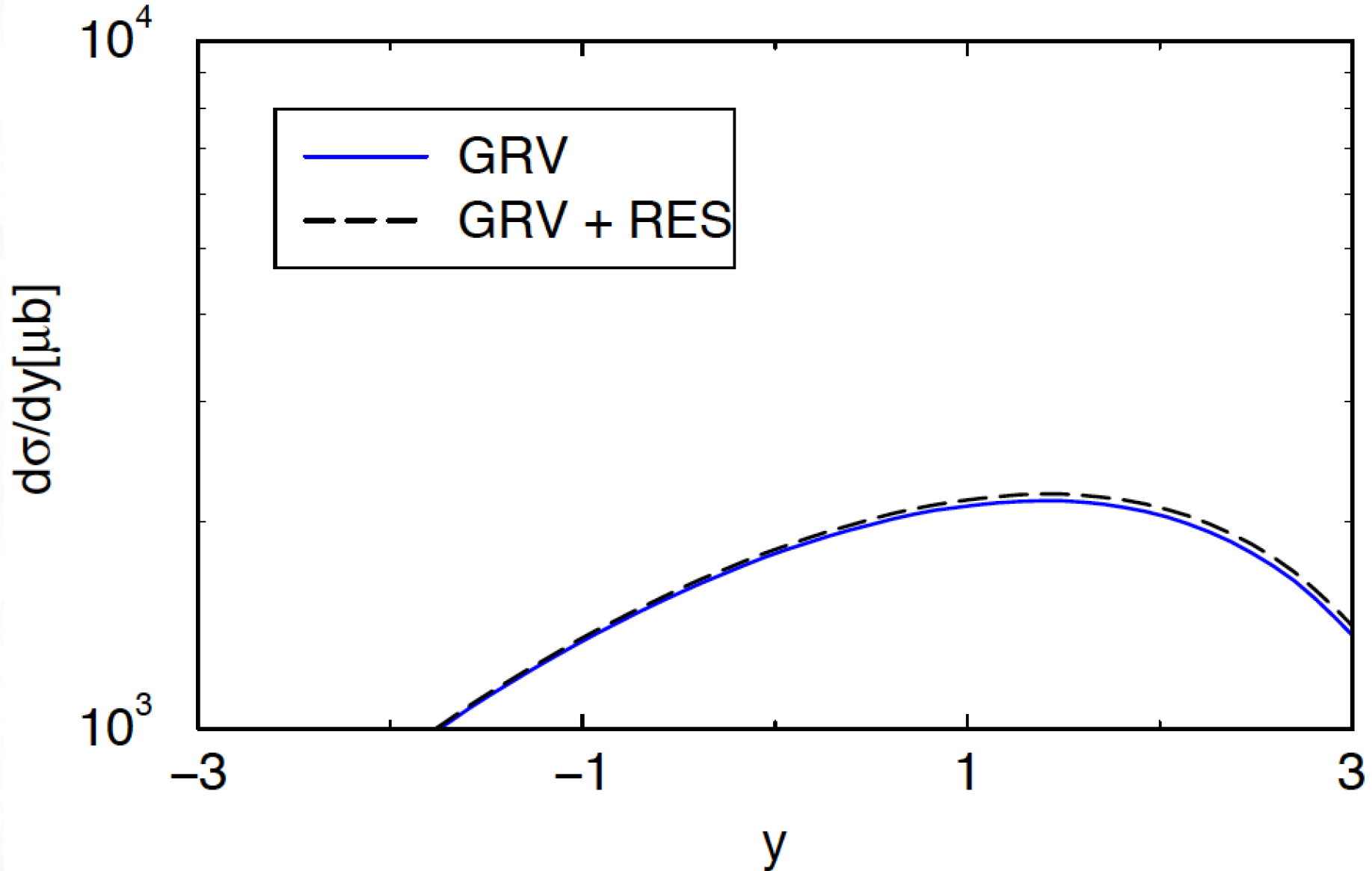
$$\sigma(AA \rightarrow XXq\bar{q}) = \int \frac{d\omega}{\omega} n(\omega) \otimes x_\gamma G_\gamma(x_\gamma, Q^2) \otimes \sigma_{gg \rightarrow q\bar{q}} \otimes x G_A(x, Q^2)$$

Glück, Owens, Reya, PRD 17, 2324 (1978)

$$\sigma_{gg \rightarrow q\bar{q}}(\hat{s}) = \frac{\pi\alpha_s^2(Q^2)}{3\hat{s}} \left[\left(1 + \epsilon + \frac{\epsilon^2}{16} \right) \ln \left(\frac{1 + \sqrt{1 - \epsilon}}{1 - \sqrt{1 - \epsilon}} \right) - \left(\frac{7}{4} + \frac{31}{16} \epsilon \right) \sqrt{1 - \epsilon} \right]$$



Resolving resolved photons



Rapidity distribution for the photoproduction of charm quarks in $^{208}\text{Pb} + ^{208}\text{Pb}$ collisions at LHC with (GRV+RES) and without (GRV) the inclusion of the resolved contribution.

J/ψ production at the LHC

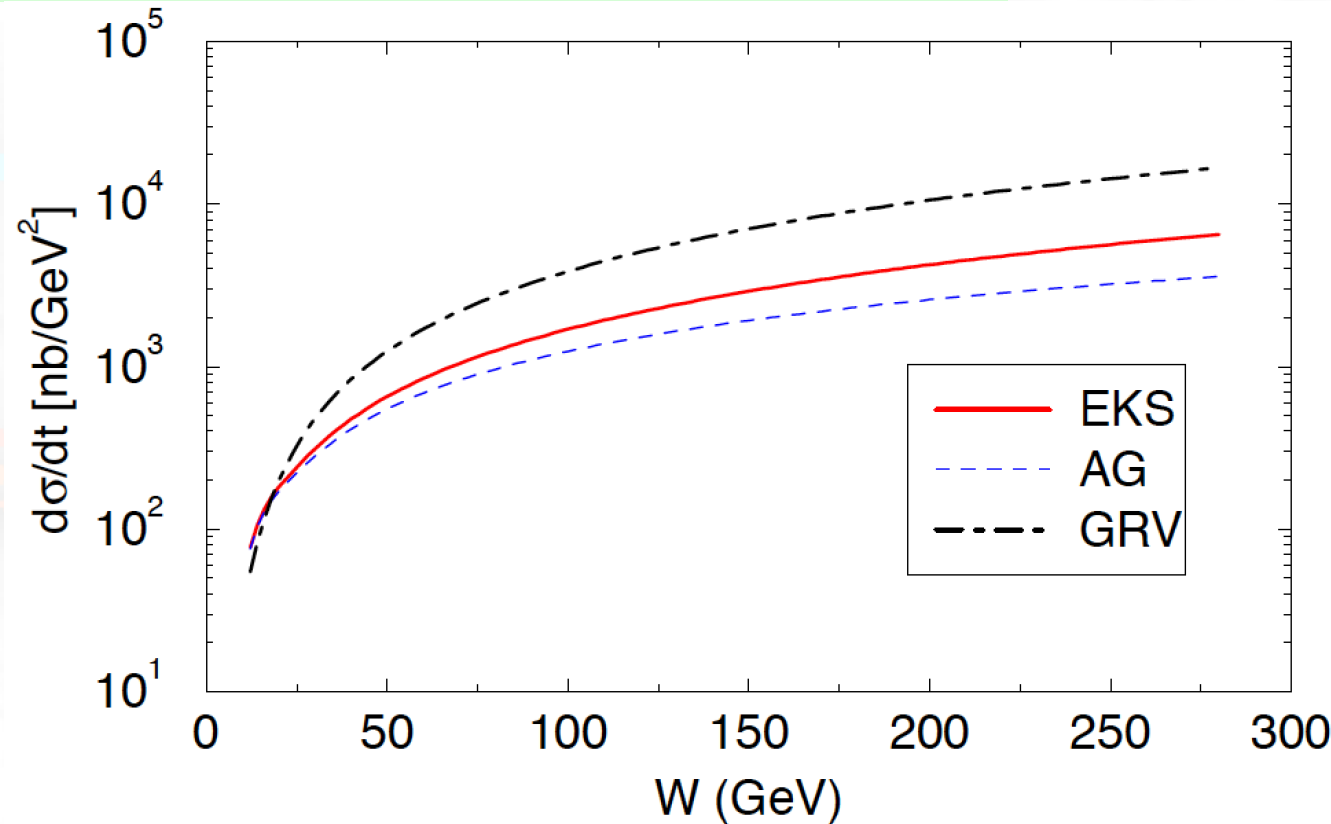
Stronger dependence on G

$$\left. \frac{d\sigma(\gamma A \rightarrow J/\psi)}{dt} \right|_{t=0} = \frac{\pi^3 \Gamma_{ee} M_{J/\psi}^3}{48\alpha} \frac{\alpha_s^2(\bar{Q}^2)}{\bar{Q}^8} \left[xG_A(x, \bar{Q}^2) \right]^2$$

$$\sigma(AA \rightarrow AAJ/\psi) = \int \frac{d\omega}{\omega} n(\omega) \int_{t_{\min}}^{\infty} dt \left. \frac{d\sigma(\gamma A \rightarrow J/\psi)}{dt} \right|_{t=0} |F(t)|^2$$

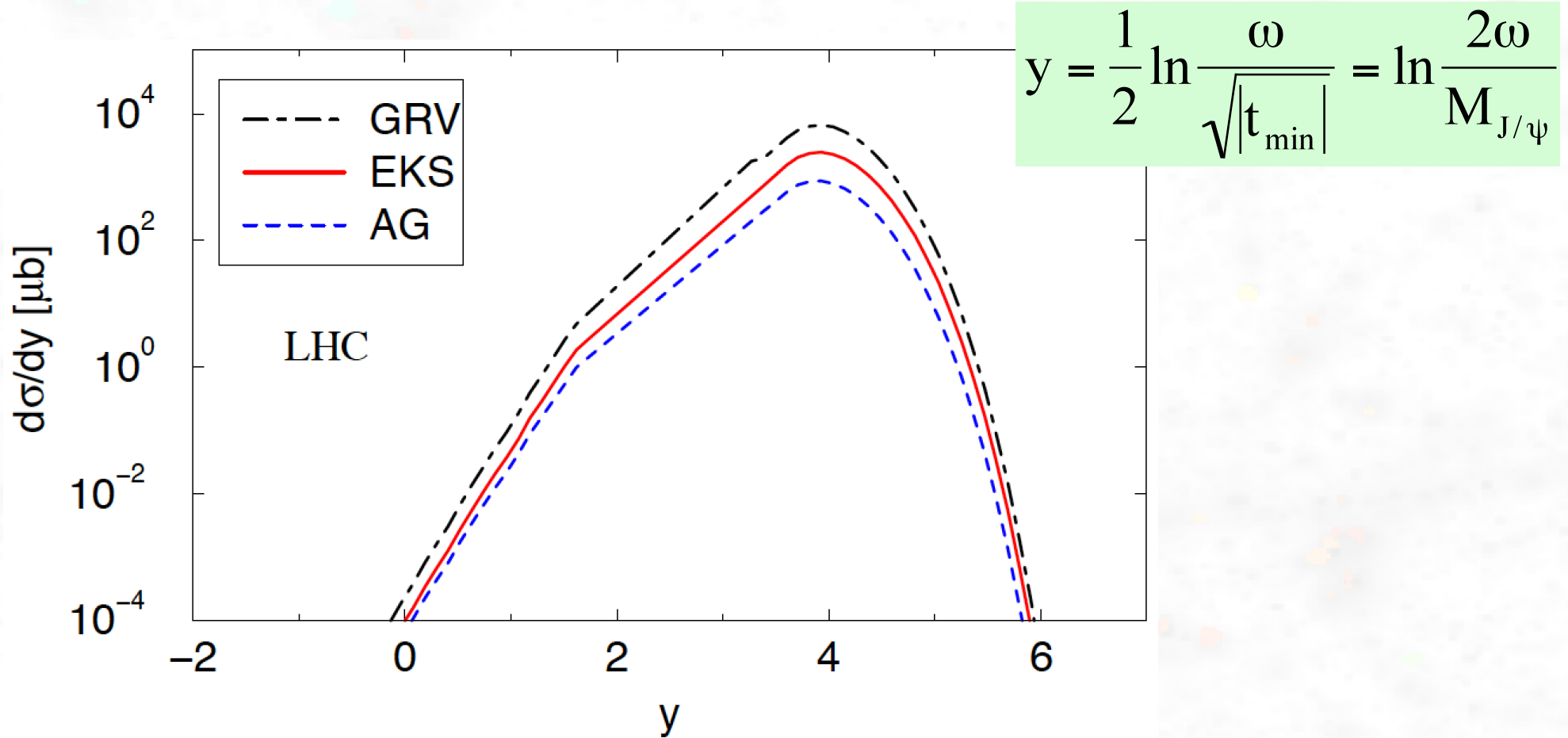
$$m_{J/\psi} = 3.097 \text{ GeV}$$

Gluon distribution	LHC
GRV	6.6 mb
EKS	2.5 mb
AG	0.9 mb



Energy dependence of the elastic photoproduction of J/ψ for distinct nuclear gluon distributions (A = 208).

J/ψ production at the LHC



The rapidity distribution for elastic photoproduction of J/ψ at LHC considering distinct nuclear gluon distributions ($A = 208$).

→ allows to estimate the magnitude of the EMC, antishadowing, and high density effects.

Nuclear modification of PDFs

Adeluyi, CB, PRC84, 024916 (2011)

$$\sigma(AA \rightarrow XXq\bar{q}) = \int \frac{dn}{d\omega}(\omega) \otimes \sigma_{\gamma g \rightarrow q\bar{q}} \otimes xG_A(x, Q^2)$$

$$xG_A(x, Q^2) = R_G \otimes xG_N(x, Q^2)$$

$x \leq 0.04$, $R_G < 1$ shadowing

$0.04 \leq x \leq 0.3$, $R_G > 1$ anti-shadowing

$0.3 \leq x \leq 0.8$, $R_G < 1$ EMC effect

$x > 0.8$, $R_G > 1$ Fermi motion

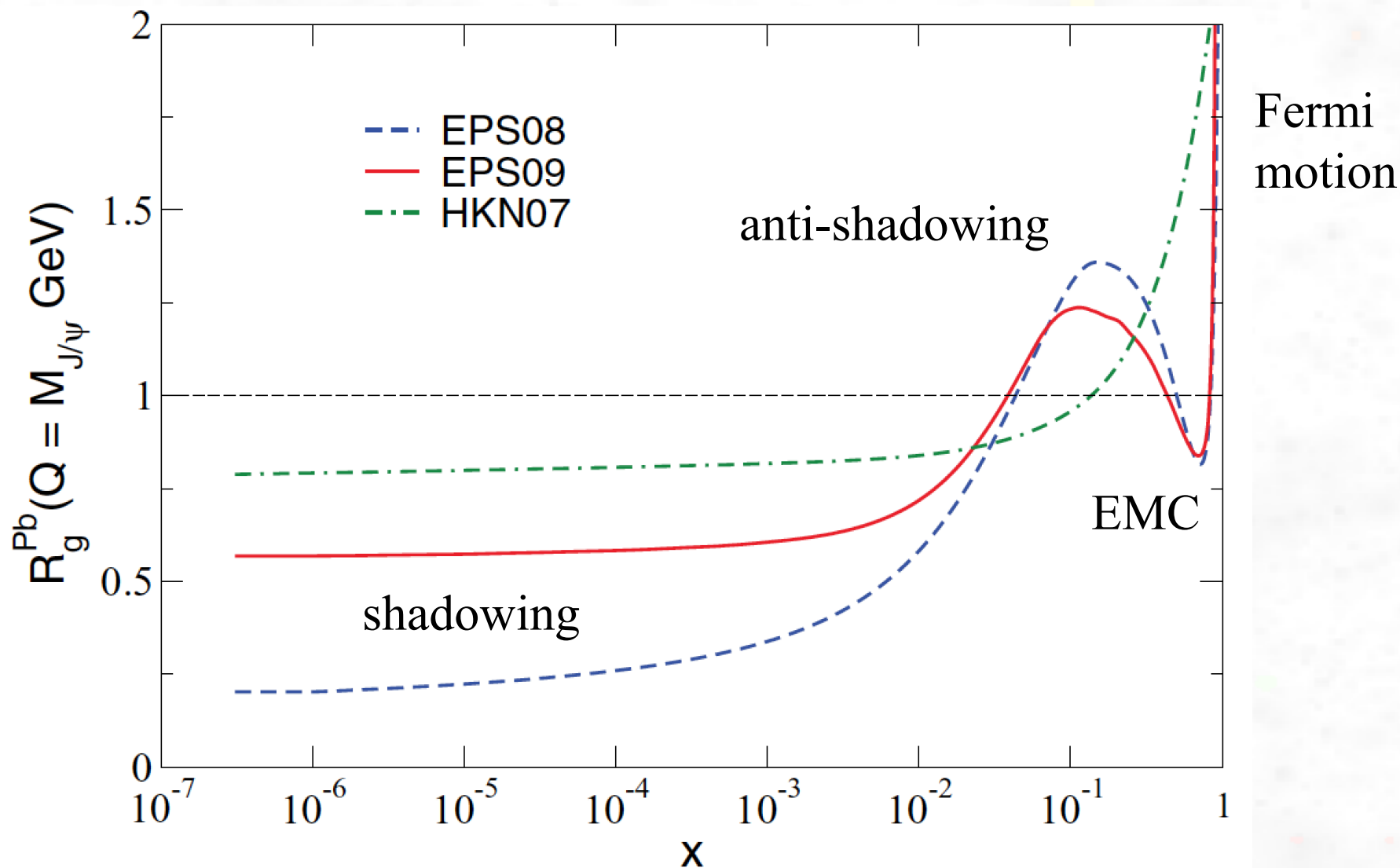


Adeola Adeluyi

Texas A&M University-Commerce

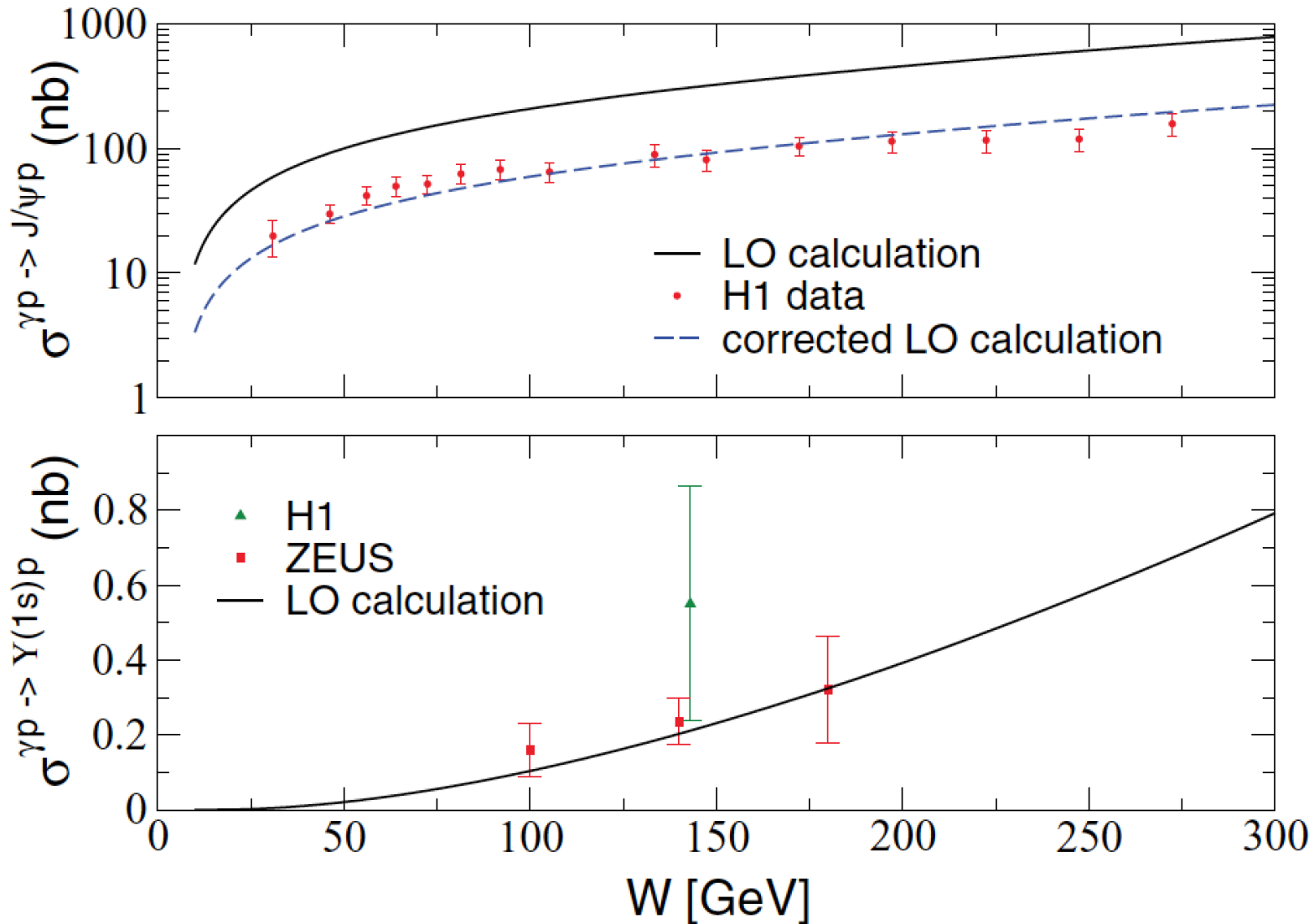
- EPS08 = Eskola, Paukunen, Salgado, JHEP 07, 102 (2008)
- EPS09 = Eskola, Paukunen, Salgado, JHEP 04, 065 (2009)
- MSTW08 = Martin, Stirling, Thorne, Watts, EPJ C 63, 189 (2009) ($R_G \sim 1$)
- HKN07 = Hirai, Kumano, Nagai, PRC 76, 065207 (2007)

Nuclear modification of PDFs



- EPS08 = Eskola, Paukunen, Salgado, JHEP 07, 102 (2008)
- EPS09 = Eskola, Paukunen, Salgado, JHEP 04, 065 (2009)
- HKN07 = Hirai, Kumano, Nagai, PRC 76, 065207 (2007)

Nuclear modification of PDFs



$\times \frac{1}{3.5}$

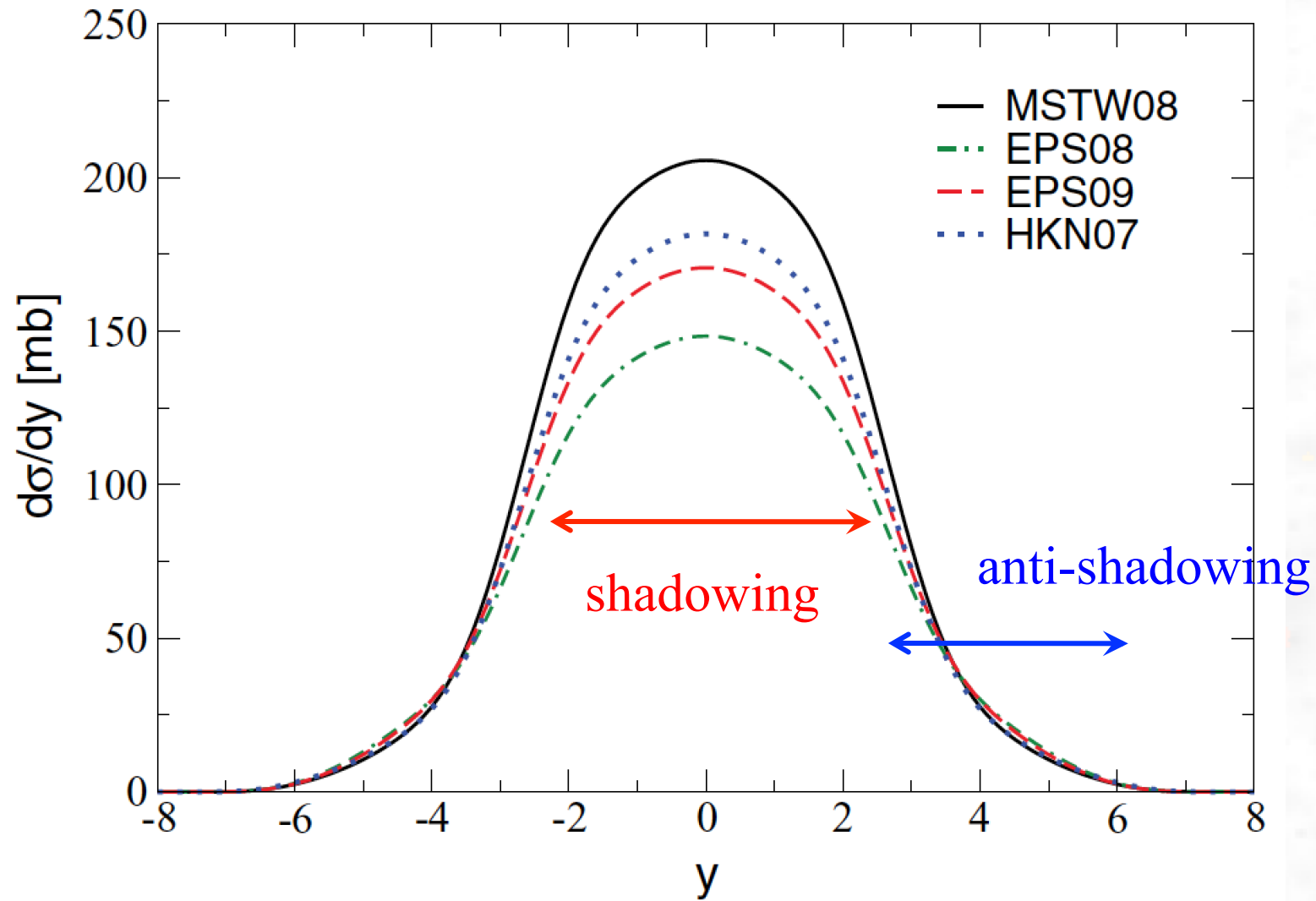
$\times 1$

Cross section for photoproduction of J/ψ (Υ) as a function of energy $W_{\gamma p}$.

$$m_{J/\psi} = 3.097 \text{ GeV}$$

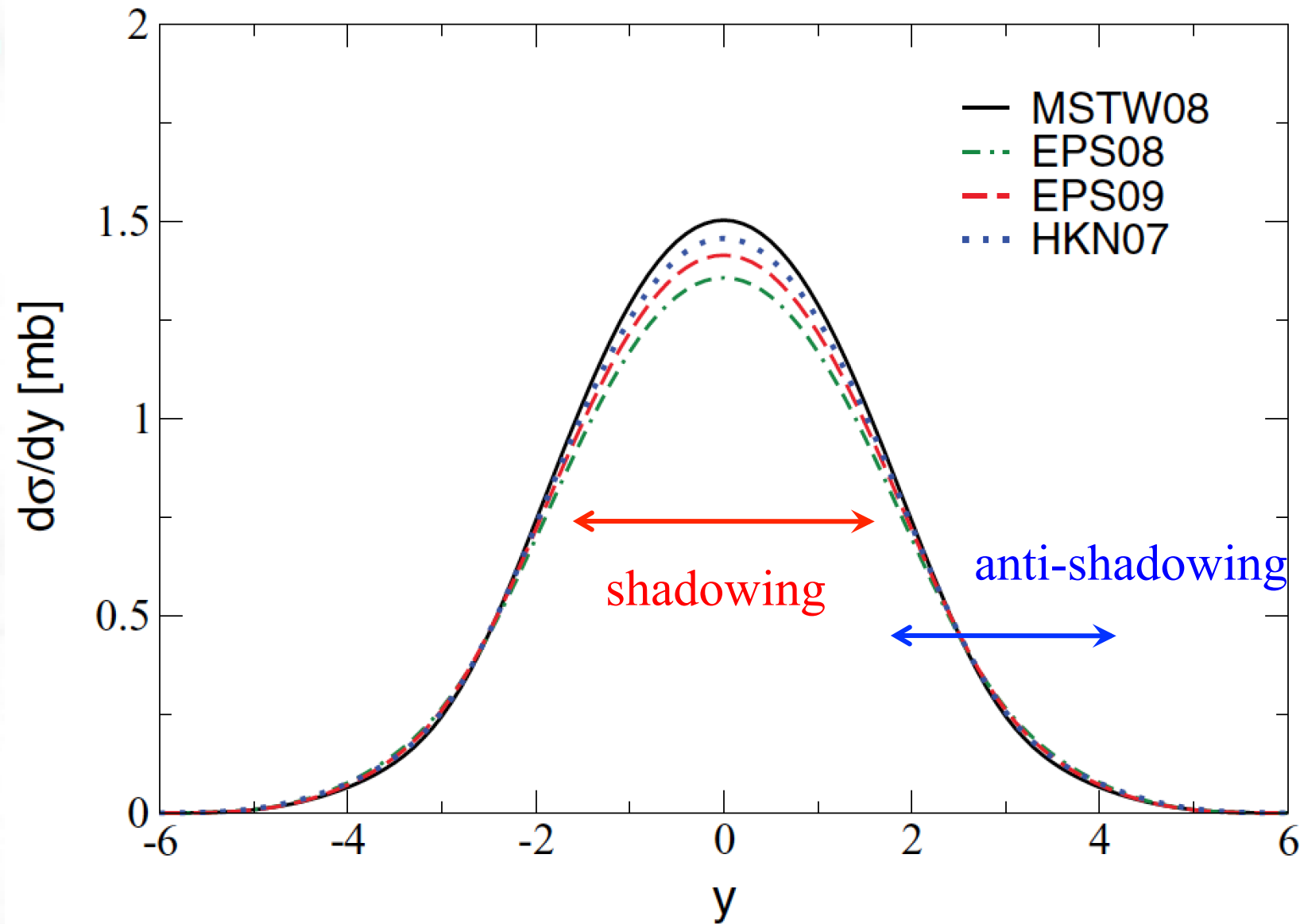
$$m_{\Upsilon} = 9.46 \text{ GeV}$$

Nuclear modification of PDFs in $c\bar{c}$ production



Total rapidity distributions of the photoproduction of $c\bar{c}$ in Pb-Pb collisions at the LHC.

Nuclear modification of PDFs in $b\bar{b}$ production



Total rapidity distributions of the photoproduction of $b\bar{b}$ in Pb-Pb collisions at the LHC.

Nuclear modification of PDFs in $q\bar{q}$ prod.

Gluon distribution	$Q^2 = s$ (mb)	$Q^2 = 4m_c^2$ (mb)
MST08	1170	1090
EPS08	890	780
EPS09	1000	910
HKN07	1080	1000

Total cross sections for direct photoproduction of $c\bar{c}$ in ultraperipheral Pb-Pb collisions at the LHC.

Gluon distribution	$Q^2 = s$ (mb)	$Q^2 = 4m_b^2$ (mb)
MST08	6.2	7.0
EPS08	5.8	6.2
EPS09	6.0	6.6
HKN07	6.1	6.7

Total cross sections for direct photoproduction of $b\bar{b}$ in ultraperipheral Pb-Pb collisions at the LHC.

Nuclear modification of PDFs at the LHC

Gluon distribution	LO (mb)	Scaled LO (mb)
MST08	260	74
EPS08	36	10
EPS09	101	29
HKN07	173	49

Total cross sections for elastic photoproduction of J/ψ in ultraperipheral Pb-Pb collisions at the LHC.

Gluon distribution	Cross section (μb)
MST08	189
EPS08	99
EPS09	130
HKN07	146

Total cross sections for elastic photoproduction of $\Upsilon(1s)$ in ultraperipheral Pb-Pb collisions at the LHC.

pA versus AA collisions

Adeluyi, CB, Murray,
PRC86, 047901 (2012)

Adeluyi, CB, PRC85, 044904 (2012)

$$\frac{dn}{d\omega} = \frac{\alpha}{2\pi\omega} \left[1 + \left(1 - \frac{2\omega}{\sqrt{s_{NN}}} \right)^2 \right] \left(\ln D - \frac{11}{6} + \frac{3}{D} - \frac{3}{2D^2} + \frac{1}{3D^3} \right)$$

Drees, Zeppenfeld,
PRD 39, 2536 (1989)

$$D = 1 + \frac{0.71 \text{ GeV}^2}{Q_{\min}^2}$$

$$Q_{\min}^2 = \frac{\omega^2}{\gamma^2 \left(1 - 2\omega / \sqrt{s_{NN}} \right)}$$

$$\sigma^X = \int d\omega \left[\frac{dn_{\gamma}^Z}{d\omega} \sigma^{\gamma p \rightarrow X}(\omega) + \frac{dn_{\gamma}^P}{d\omega} \sigma^{\gamma A \rightarrow X}(\omega) \right]$$

$$\sigma_{q\bar{q} \rightarrow Q\bar{Q}}(\hat{s}) = \frac{8\pi\alpha_s^2(Q^2)}{27\hat{s}} \left[\left(1 + \frac{\varepsilon}{2} \right) \sqrt{1 - \varepsilon} \right] \quad \hat{s} = x_1 x_2 s$$

Combridge, Nucl. Phys. B 151, 429 (1979)



Michael Murray
U. of Kansas

Photon PDFs for resolved interactions:

- GRV = Glück, Reya, Vogt, Phys. Rev. D 46, 1973 (1992)
- SaS1d = Schuler, Sjostrand, Z. Phys. C 68, 607 (1995)
- CJK2 = Cornet, Jankowski, Krawczyk, Acta Phys. Pol. B 35, 2215 (2004)

pA versus AA collisions

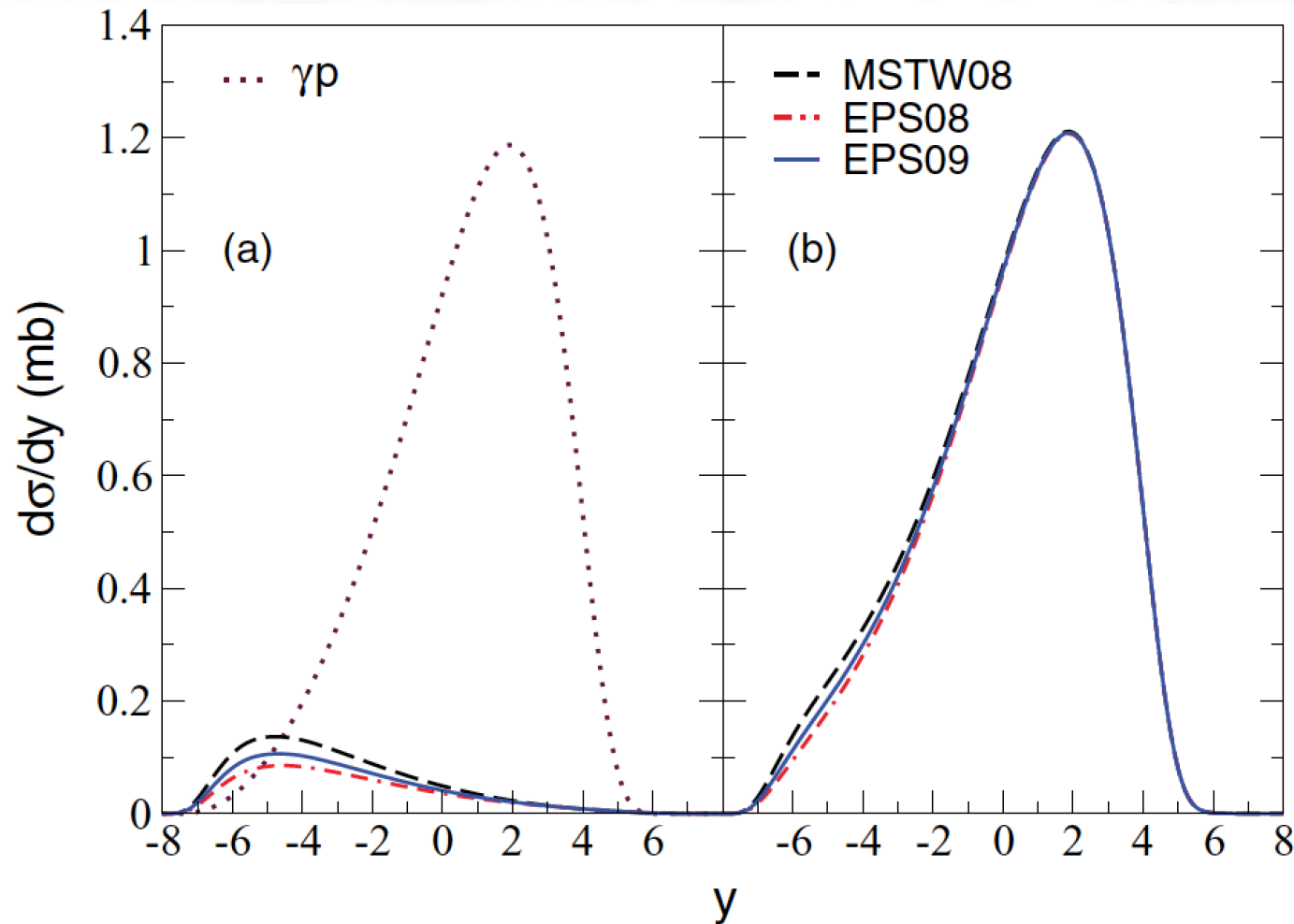
	PDF	direct	SaS1d	Resolved GRV	CJK
γp	MSTW08	5570	692	1157	1418
	MSTW08	607	114	195	228
γA	EPS08	376	95	164	187
	EPS09	471	103	177	204

Cross sections for photoproduction of $c\bar{c}$ in ultraperipheral pPb collisions at the LHC. All cross sections are in **microbarns (μb)**.

	PDF	direct	SaS1d	Resolved GRV	CJK
	MSTW08	1167	110	180	226
	EPS08	890	104	172	213
	EPS09	1002	106	176	219

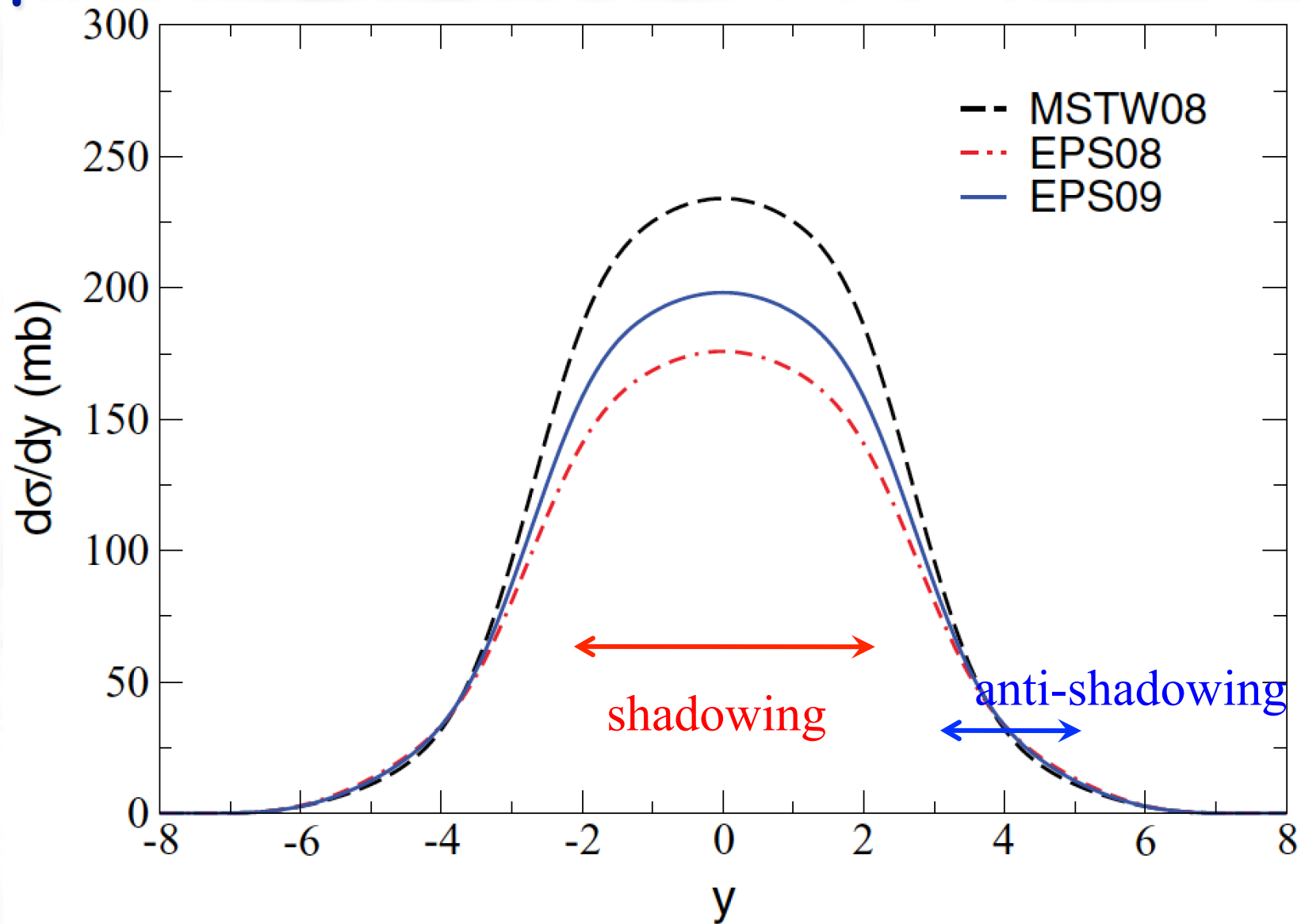
Cross sections for photoproduction of $c\bar{c}$ in ultraperipheral PbPb collisions at the LHC. All cross sections are in **millibarns (mb)**.

pA versus AA collisions



Rapidity distributions of $c\bar{c}$ photoproduction in pPb collisions at the LHC using the GRV photon parton distributions. In (a) we show the γp and γPb contributions to total rapidity distributions. Dotted line depicts the γp contribution, while the dashed (MSTW08), solid (EPS09), and dash-dotted (EPS08) lines correspond to γPb contributions. In (b) we present total rapidity distributions (sum of γp and γPb contributions).

pA versus AA collisions



Total rapidity distributions of the photoproduction of $c\bar{c}$ in PbPb collisions at the LHC using the GRV photon parton distributions. Dashed line depicts result using the MSTW08 gluon distribution. Solid and dash-dotted lines are results from nuclear-modified gluon distributions from EPS09 and EPS08.

pA versus AA collisions

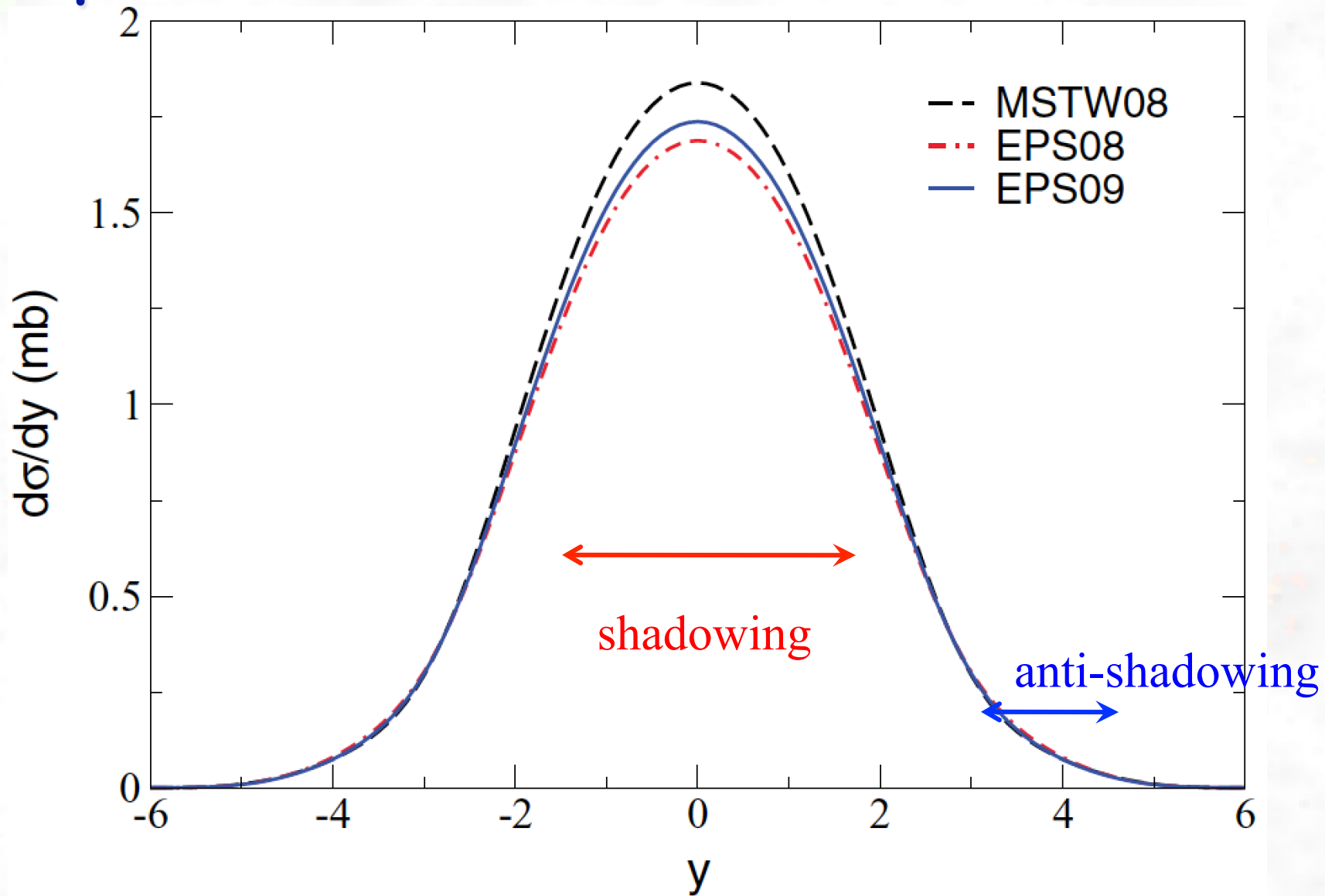
	PDF	direct	SaS1d	Resolved GRV	CJK
yp	MSTW08	36512	8641	112178	114977
	MSTW08	5084	2061	3032	3663
yA	EPS08	3972	1936	2872	3451
	EPS09	4409	1988	2942	3543

Cross sections for photoproduction of $b\bar{b}$ in ultraperipheral pPb collisions at the LHC. All cross sections are in **nanobarns (nb)**.

	PDF	direct	SaS1d	Resolved GRV	CJK
	MSTW08	6227	1076	1468	1800
	EPS08	5812	1097	1516	1867
	EPS09	5992	1085	1496	1842

Cross sections for photoproduction of $b\bar{b}$ in ultraperipheral PbPb collisions at the LHC. All cross sections are in **microbarns (μb)**.

pA versus AA collisions



Total rapidity distributions of $b\bar{b}$ photoproduction in PbPb collisions at the LHC using the GRV photon PDF. Dashed line depicts result using the MSTW08 gluon distribution (no nuclear modifications). Solid and dash-dotted lines are results from nuclear-modified distributions from EPS09 and EPS08.

pA versus AA collisions

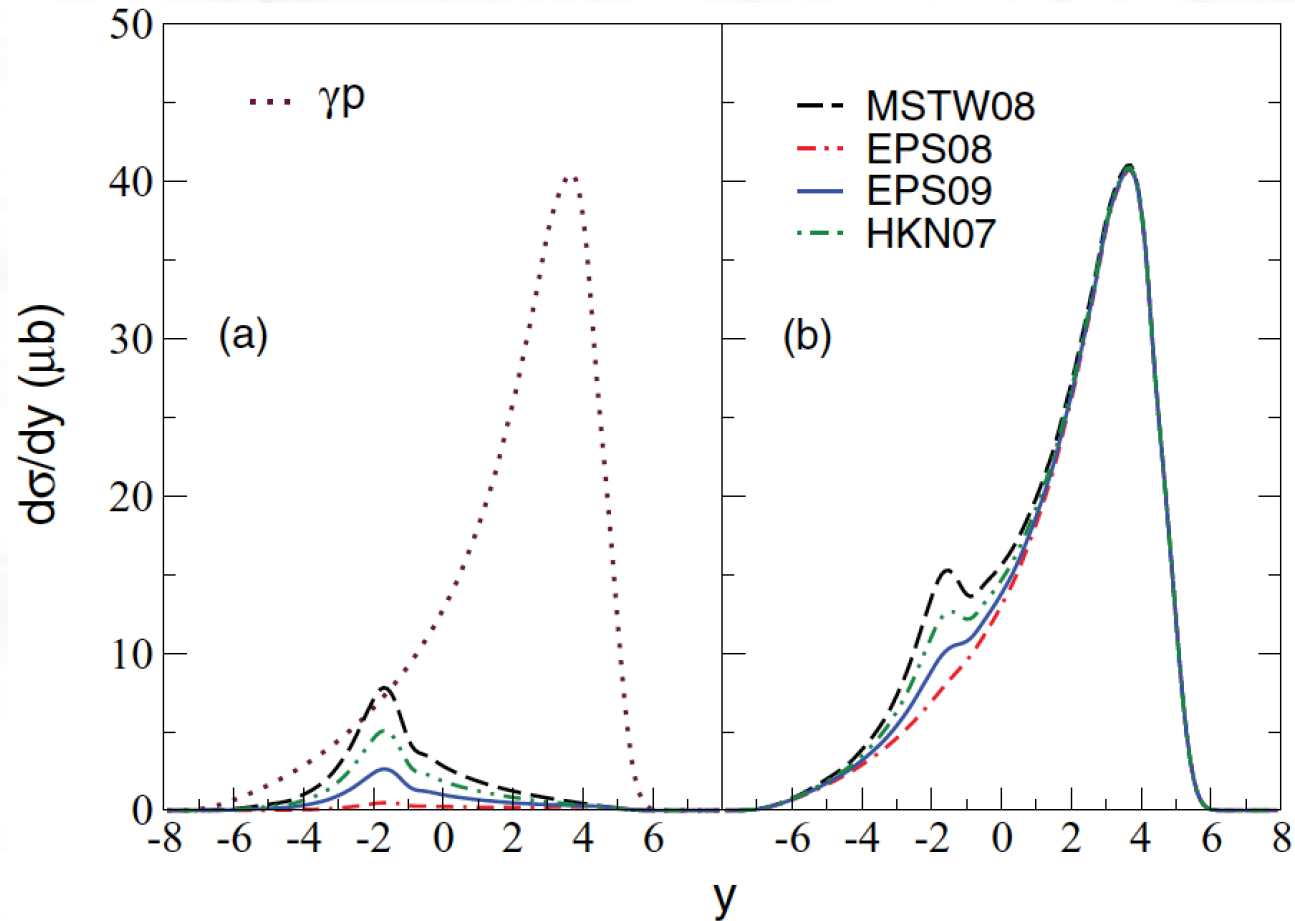
	γp	γA	total
MSTW08	167.3	23.6	190.9
EPS08		2.2	169.5
EPS09		8.5	175.8
HKN07		15.4	182.7

Cross sections (**in μb**) for elastic photoproduction of J/ψ in ultraperipheral pPb collisions at the LHC. Second and third columns are the contributions from γp and γPb . The sums of the two contributions are presented in the fourth column.

	Cross section (μb)
MSTW08	74
EPS08	10
EPS09	29
HKN07	49

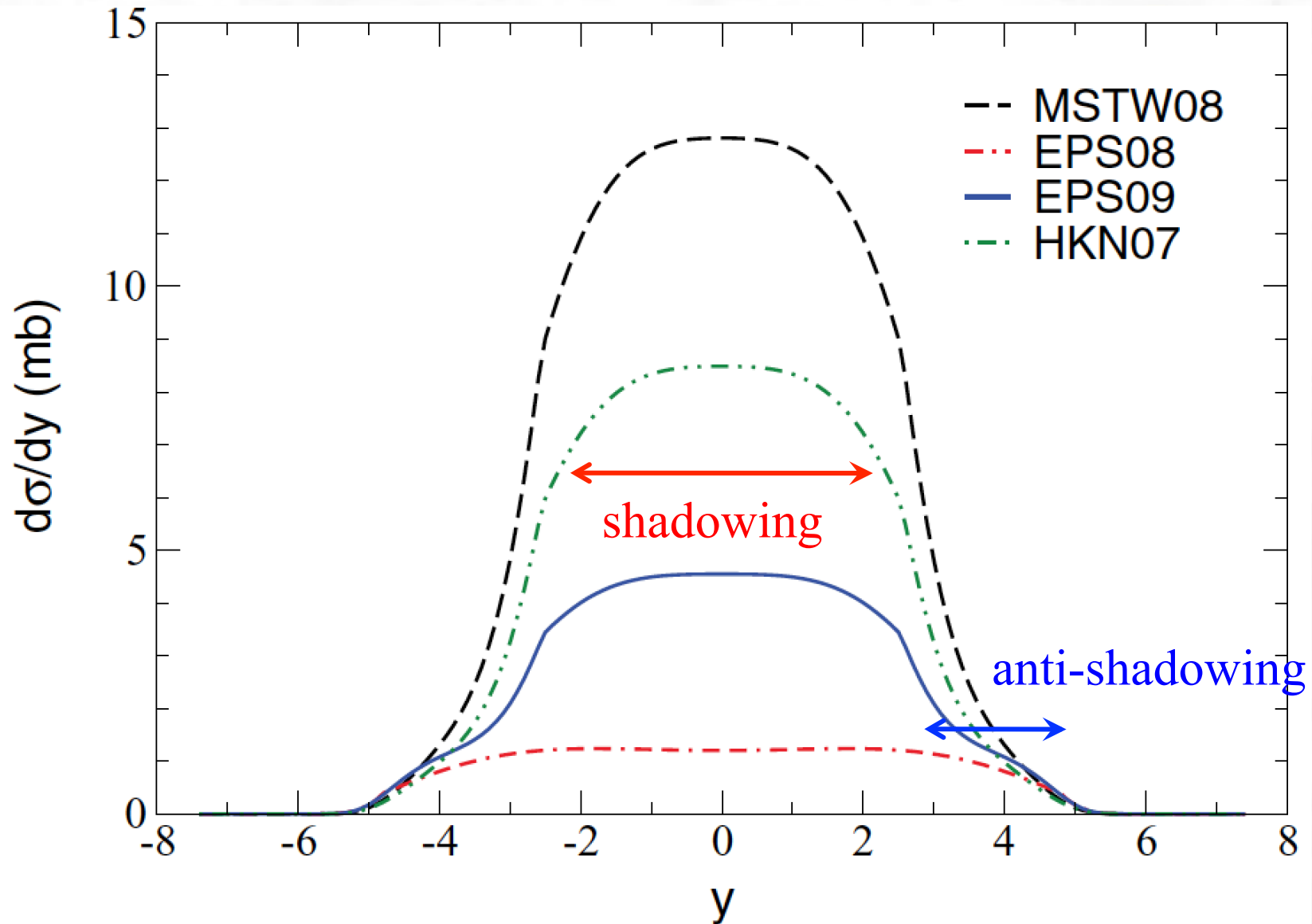
Total cross sections (**in mb**) for elastic photoproduction of J/ψ in ultraperipheral PbPb collisions at the LHC.

pA versus AA collisions



Rapidity distributions of exclusive photoproduction of J/ψ in pPb collisions at the LHC. In (a) we show the γp and γPb contributions to total rapidity distributions. Dotted line depicts the γp contribution while the dashed (MSTW08), dash double-dotted (HKN07), solid (EPS09), and dash-dotted (EPS08) lines correspond to γPb contributions with no shadowing, weak shadowing, moderate shadowing, and strong shadowing, respectively. In (b) we present total rapidity distributions (sum of γp and γPb contributions).

pA versus AA collisions



Total rapidity distributions of exclusive photoproduction of J/ψ in PbPb collisions at the LHC. Dashed line depicts results using the MSTW08 gluon distribution. Solid, dash-dotted, and dash-double-dotted lines are results from nuclear-modified gluon distributions from EPS09, EPS08, and HKN07.

pA versus AA collisions

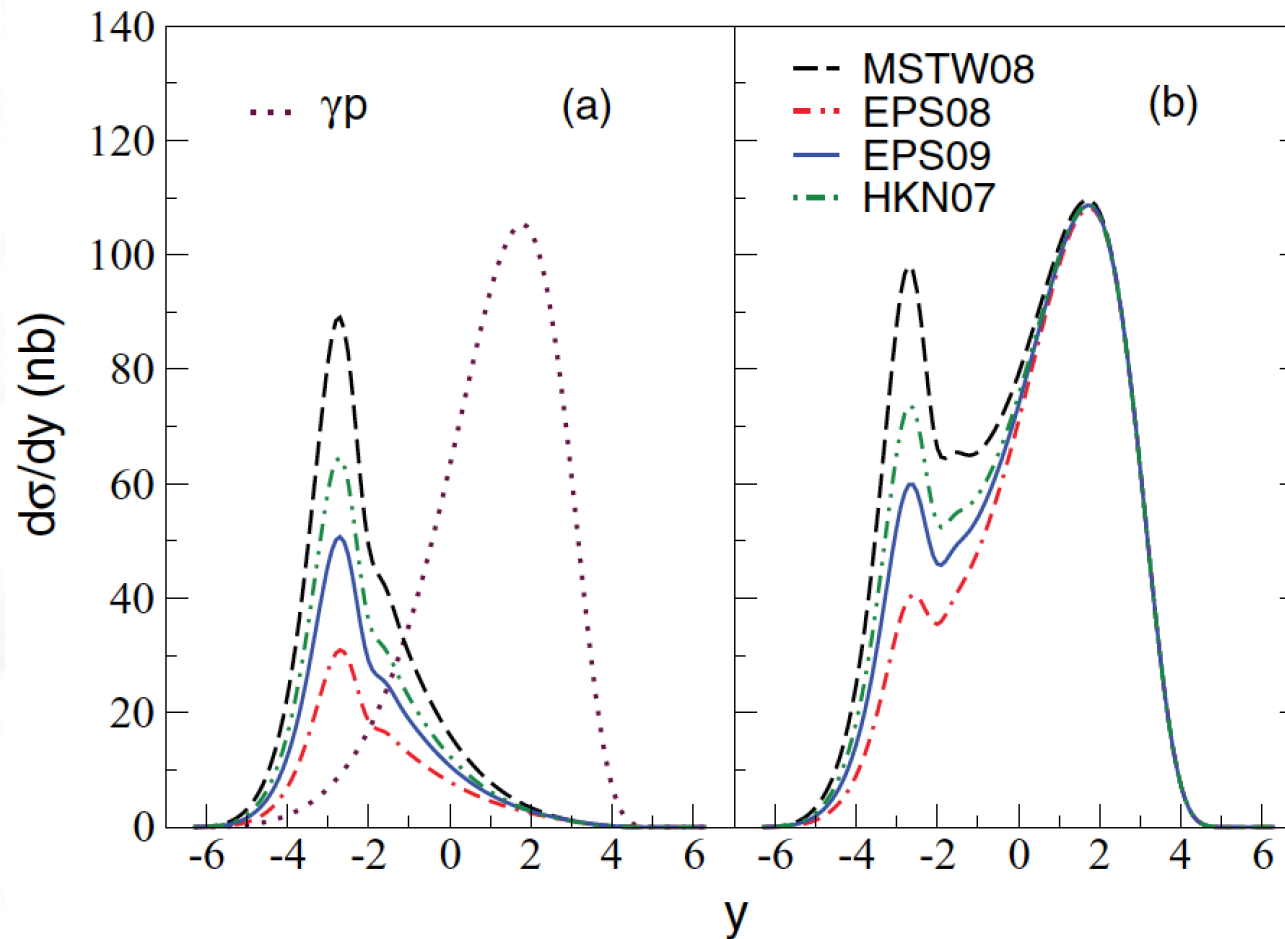
	γp	γA	total
MSTW08	390	219	609
EPS08		84	474
EPS09		130	520
HKN07		161	551

Total cross sections (**in nb**) for elastic photoproduction of $\Upsilon(1s)$ in ultraperipheral pPb collisions at the LHC. Second and third columns are the contributions from γp and γPb . The sums of the two contributions are presented in the fourth column.

	Cross section
MSTW08	189
EPS08	99
EPS09	130
HKN07	146

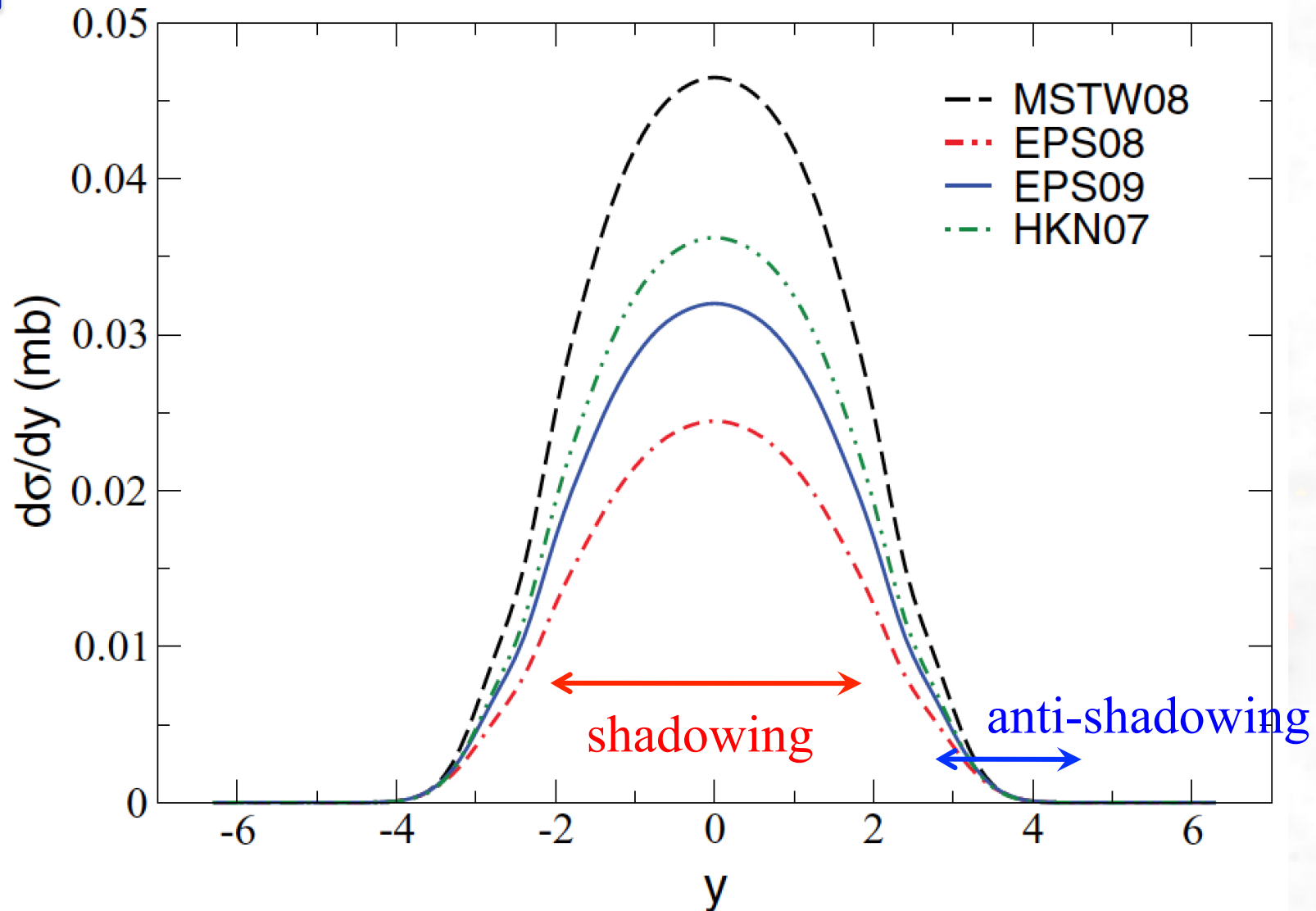
Total cross sections (**in μb**) for elastic photoproduction of $\Upsilon(1s)$ in ultraperipheral PbPb collisions at the LHC.

pA versus AA collisions



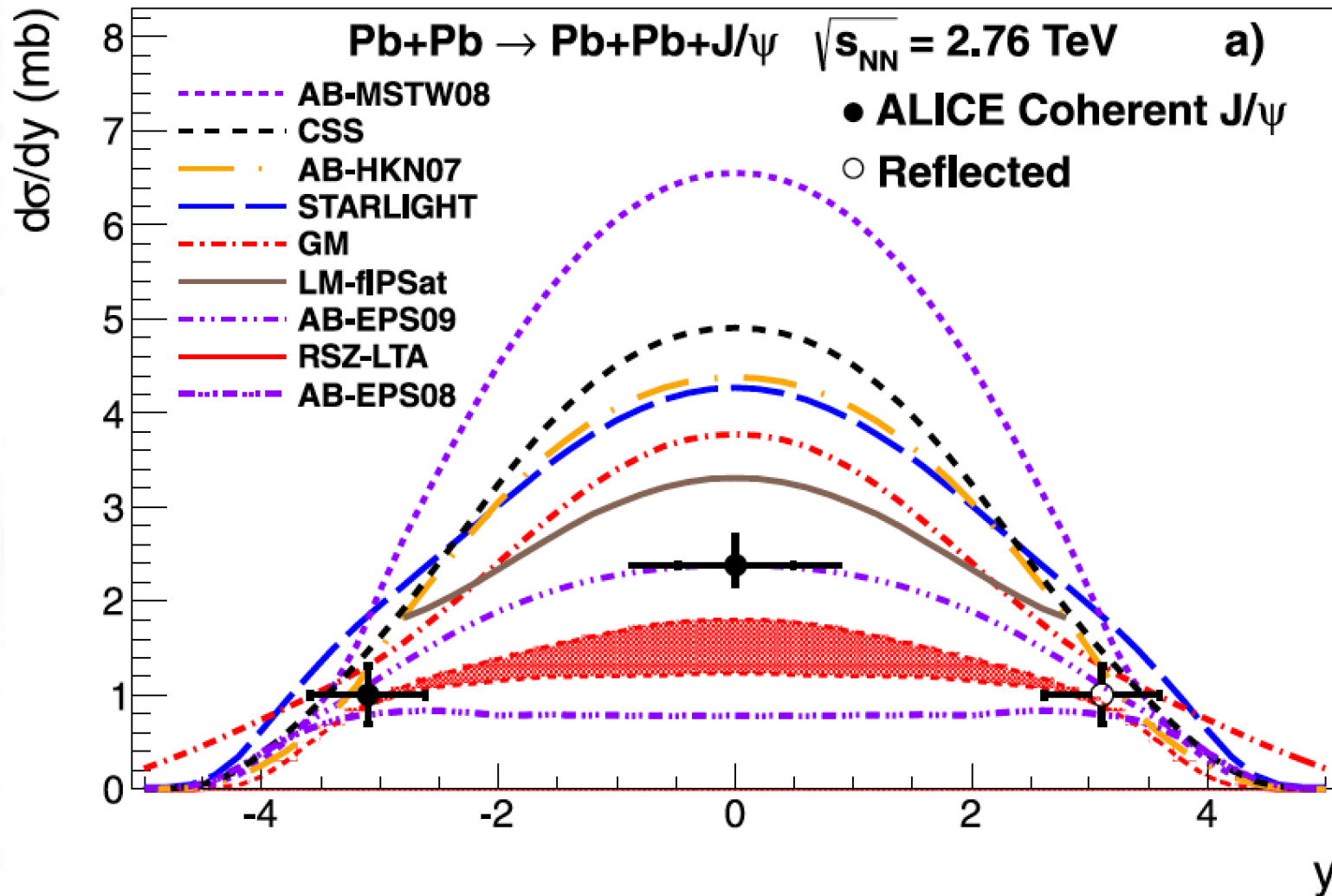
Rapidity distributions of exclusive photoproduction of $\Upsilon(1s)$ in pPb collisions at the LHC. In (a) we show the γp and γPb contributions to total rapidity distributions. Dotted line depicts the γp contribution while the dashed (MSTW08), dash double-dotted (HKN07), solid (EPS09), and dash-dotted (EPS08) lines correspond to γPb contributions with no shadowing, weak shadowing, moderate shadowing, and strong shadowing, respectively. In (b) we present total rapidity distributions (sum of γp and γPb contributions).

pA versus AA collisions



Total rapidity distributions of exclusive photoproduction of $\Upsilon(1s)$ in PbPb collisions at the LHC in the modified hard sphere density distribution approximation. Dashed line depicts result using the MSTW08 gluon distribution. Solid, dash-dotted, and dash-double-dotted lines are results from nuclear-modified gluon distributions from EPS09, EPS08, and HKN0.

PDFs at the LHC



De Gruttola et al., NPA (2014)

Comparison among the published value of the cross section at forward rapidity, the result at central rapidities and several theoretical models. The error is the quadratic sum of the statistical and systematic errors.

Summary

- Don't steal particle accelerators from physics beyond the SM
- However, they can be very useful for complementary studies (e.g. $\gamma^* + \Lambda \rightarrow \Sigma^0$ and Σ^0 lifetime)
 - Witnesses:
 - antihydrogen (CERN 1996)
 - multiphonon giant resonances (GSI 1992)
 - alternatives for nuclear astrophysics (everywhere but CERN)
 - QFT of bound states (nowhere)
 - PDFs (RHIC, CERN)

• • •